A Review of Piezoelectric Energy Harvesting: Materials, Design, and Readout Circuits

actuators

MDPI

Review

A Review of Piezoelectric Energy Harvesting: Materials, Design, and Readout Circuits

Eugenio Brusa *, Anna Carrera and Cristiana Delprete

Department of Mechanical and Aerospace Engineering (DIMEAS), Politecnico di Torino, Corso Duca Degli Abruzzi 24, 10129 Torino, Italy; anna.carrera@polito.it (A.C.); cristiana.delprete@polito.it (C.D.)
* Correspondence: eugenio.brusa@polito.it

Abstract: Mechanical vibrational energy, which is provided by continuous or discontinuous motion, is an infinite source of energy that may be found anywhere. This source may be utilized to generate electricity to replenish batteries or directly power electrical equipment thanks to energy harvesters. The new gadgets are based on the utilization of piezoelectric materials, which can transform vibrating mechanical energy into useable electrical energy owing to their intrinsic qualities. The purpose of this article is to highlight developments in three independent but closely connected multidisciplinary domains, starting with the piezoelectric materials and related manufacturing technologies related to the structure and specific application; the paper presents the state of the art of materials that possess the piezoelectric property, from classic inorganics such as PZT to lead-free materials, including biodegradable and biocompatible materials. The second domain is the choice of harvester structure, which allows the piezoelectric material to flex or deform while retaining mechanical dependability. Finally, developments in the design of electrical interface circuits for readout and storage of electrical energy given by piezoelectric to improve charge management efficiency are discussed.

Keywords: piezoelectric; energy harvesting; renewable energies; piezoelectric structure; piezoelectric design; piezoelectric materials; bimorph harvester; harvesting circuit; electric circuit

Citation: Brusa, E.; Carrera, A.; Delprete, C. A Review of Piezoelectric Energy Harvesting: Materials, Design, and Readout Circuits. *Actuators* **2023**, *12*, 457. https://doi.org/10.3390/act12120457

Academic Editors: Hongli Ji and Yi-Chung Shu

Received: 30 September 2023
Revised: 26 November 2023
Accepted: 5 December 2023
Published: 8 December 2023

1. Introduction

The use of electronic devices has grown swiftly and continues to rise rapidly as technology advances. Electronic equipment is often powered by electrical outlets or batteries. The increased use of nonrenewable energy sources, such as batteries, has resulted in increased pollution and the emergence of severe energy crisis scenarios. Batteries have a substantial environmental impact when they are disposed of, in addition to having a limited lifespan that is generally shorter than that of electronic devices. This is an important issue nowadays because, in addition to requiring frequent recharging and replacement, they can also be found in difficult-to-access areas or disrupt the manufacturing cycle. In an industrial environment, for example, replacing batteries in nodes with sensors on machines that monitor the manufacturing process causes downtime, waste that reduces production efficiency, delays, and increased maintenance costs. Consider changing batteries in difficult-to-reach locations such as the middle of the sea or in devices implanted in the human body, as well as the associated expenses. Energy harvesters are considered among the most promising technologies to overcome battery-induced difficulties due to qualities such as miniaturization, high computational power, multi-functionality, and low-power communication [1–4].

Energy harvesters are devices or systems that gather and transform ambient energy from their surroundings into electrical energy. They are also known as energy scavengers or power harvesters. The energy harvested can be used to power small electronic devices or charge batteries, reducing battery replacement and the need for traditional power outlets. Energy harvesters are especially beneficial in isolated or difficult-to-reach areas

where changing or charging batteries is impractical. Energy harvesters range in size and complexity, from micro-scale devices to power sensors to bigger systems capable of generating significant amounts of electricity. Their efficiency is determined by the type of energy source and technology employed. Energy harvesting technologies are being developed and improved by researchers and engineers to make them more efficient, dependable, and usable in a variety of industries, including IoT (Internet of Things), wireless communication, remote sensing, and biomedical applications. The latter, primarily in the form of wearable sensors, enable monitoring of human health and physiological performance by nonintrusive, continuous, and real-time assessment of human physiological parameters [5–11]. Depending on the type of energy conversion, nanogenerators can be classified as piezoelectric nanogenerators (PENG) [12–14], triboelectric nanogenerators (TENG) [15–19], pyroelectric nanogenerators (PYNG) [20], thermoelectric [21,22], and solar cells [23,24].

Depending on the application and energy need, energy harvesters may draw on a variety of environmental energy sources. Figure 1 includes information about each of them [25–30].

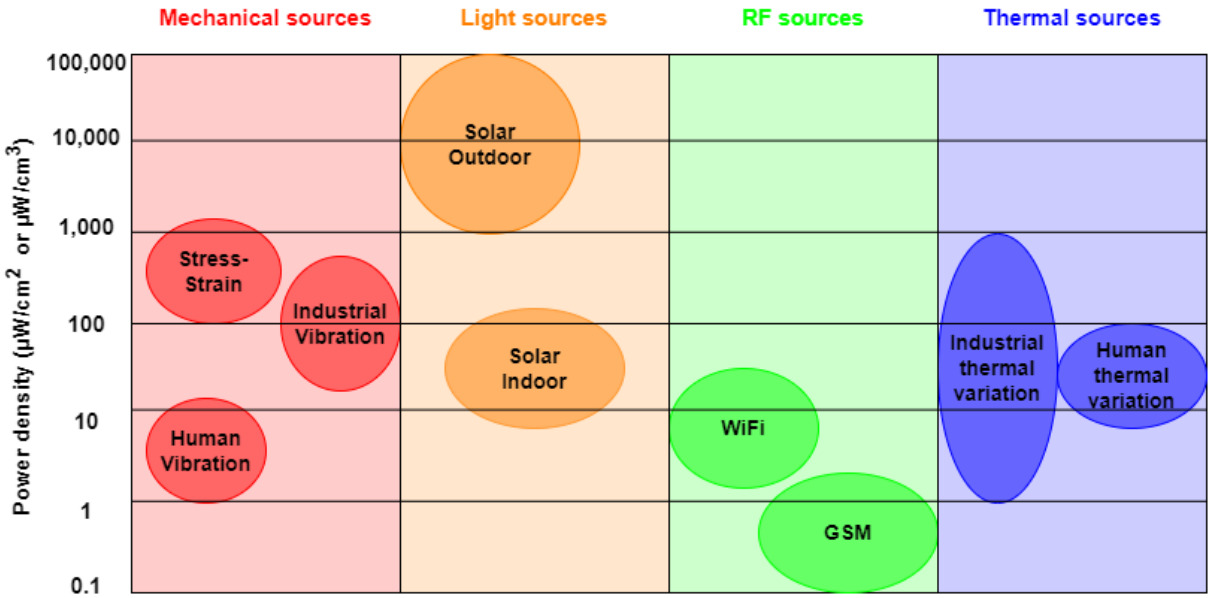

Figure 1. Power density of energy harvested from the different types of energy harvesting sources available.

Mechanical energy is the most common of the sources discussed since continuous or intermittent mechanical motion is an energy that is present and available to everyone in everyday life [31,32]. Mechanical energy harvesters typically use electromagnetic, electrostatic, and piezoelectric systems [32–34]. The last environmental energy harvesting technology is the most promising.

Erturk and Inman [35] have defined piezoelectricity as "a form of coupling between the mechanical part and the electrical behaviors of ceramics and crystals belonging to certain classes". Piezoelectric energy harvesting is the conversion of mechanical energy, such as vibration, strain, or pressure, into electrical energy using the piezoelectric principle. This idea is based on the capacity of some materials, known as piezoelectric materials, to create an electrical potential difference when subjected to mechanical stress. Piezoelectric generators are tiny and compact, and they may be easily incorporated into micro-electromechanical systems. Moreover, they are unaffected by environmental conditions such as humidity [36,37]. Piezoelectric generators are more reliable, have a longer lifetime, are more sensitive to low stresses, and generate a far greater charge density and voltage output than other energy harvesting systems [12,38–42]. The quality of the piezoelectric material employed, the

frequency and intensity of vibration or strain, and the system design and management of the charge collected from the piezoelectric generator all influence the effectiveness of piezoelectric energy harvesting. We emphasize the most relevant factors in the design of a piezoelectric energy harvester in the schematic displayed in Figure 2.

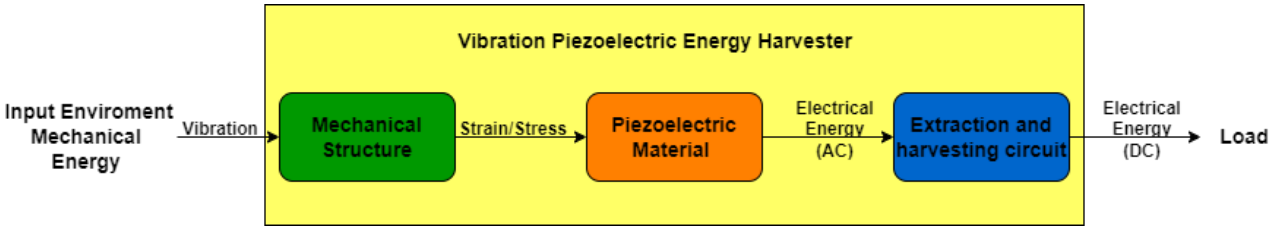

Figure 2. Architecture of the vibration energy harvesting chain from source to user.

Section 2, then, delves into the technology that characterizes piezoelectricity, and the classification of piezoelectric materials based on their origin and usage. In Section 3, this review attempts to categorize the many forms of structural layouts that characterize piezoelectric vibration energy harvesters (PVEHs), from the most traditional to the most creative. Section 4 presents the various electronic interface circuits used in extracting and managing the electrical energy delivered by the piezoelectric generator.

2. Materials

Piezoelectric materials are a type of material that may create an electrical charge in reaction to mechanical stress or deformation, as well as undergo mechanical deformation when exposed to an electric field. The piezoelectric effect is a reversible feature of this characteristic. When a piezoelectric material is subjected to mechanical force or stress, the locations of charged atoms or ions inside the material's crystal lattice structure alter. This charge transfer causes an electrical potential or voltage to be generated across the substance. It is possible to distinguish between the direct and reverse piezoelectric effects [43–45]. When mechanical stress causes a buildup of electrical charge in a material, the direct piezoelectric effect occurs. This effect is widely employed in a variety of applications, including piezoelectric sensors and transducers. The inverse of the direct effect is the reverse piezoelectric effect. When a piezoelectric material is subjected to an electric field, it deforms or changes shape. This phenomenon is employed in piezoelectric actuators and motors. Piezoelectricity is found in materials that lack the center of symmetry and have a total dipole moment other than zero. A piezoelectric material has three operating modes. Mode d_{33}, also known as longitudinal mode, is the operating mode in which the polarization and stress directions are parallel; it is recommended for applications such as piezoelectric energy harvesting. The d_{31} mode, also known as the transverse mode, is the mode in which the polarization and applied stress directions are perpendicular to one other. The third mode is parallel shear mode d_{15}, which occurs when charge is collected on electrodes perpendicular to the initial polarization electrodes and shear mechanical force is applied [46]. This property is not inherent in all materials labeled as piezoelectric. To gain the property, ferroelectrics must be polarized. Figure 3 depicts a first categorization [47].

Ferroelectric materials, despite enjoying high electromechanical processing efficiency and good manufacturability, are subject to the following:

- Depolarization occurs when materials are exposed to the following conditions: high electric fields in the opposite direction of the polarizing field or high alternating electric fields.
  - Significant mechanical stresses;
  - Above the so-called Curie temperatures, a phase change in the crystal structure occurs, resulting in the loss of piezoelectric characteristics.
- Aging: the loss of piezoelectric capabilities with time as one advances away from the moment of polarization.

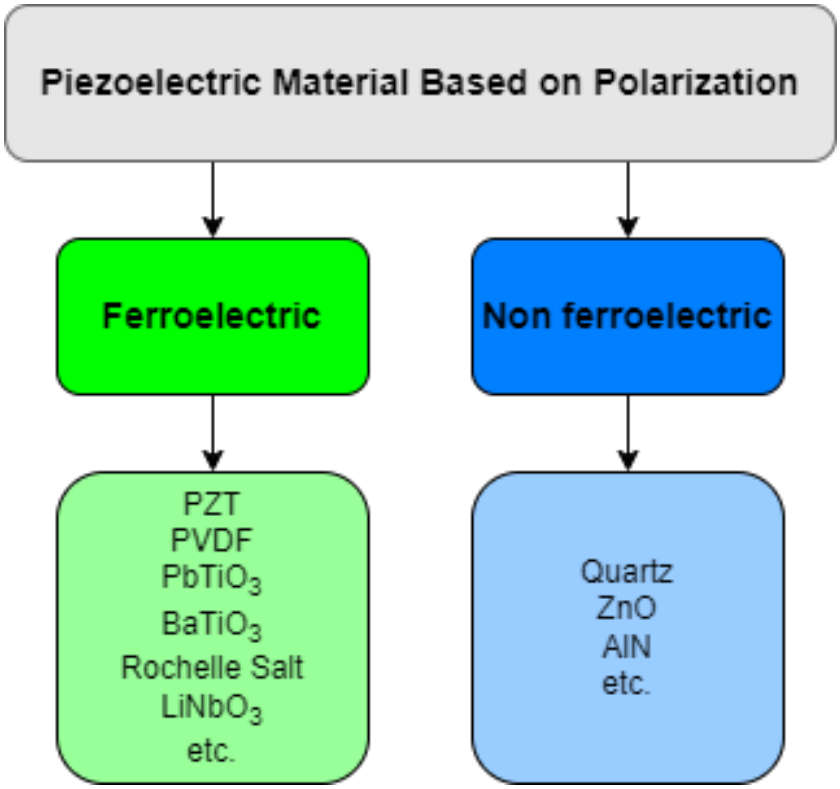

Figure 3. Preliminary classification of piezoelectric materials currently used in engineering applications into ferroelectric and non-ferroelectric materials.

This section compares and examines the various subclasses of synthetic piezoelectric materials (ceramics, polymers, and composites), as seen in Figure 4.

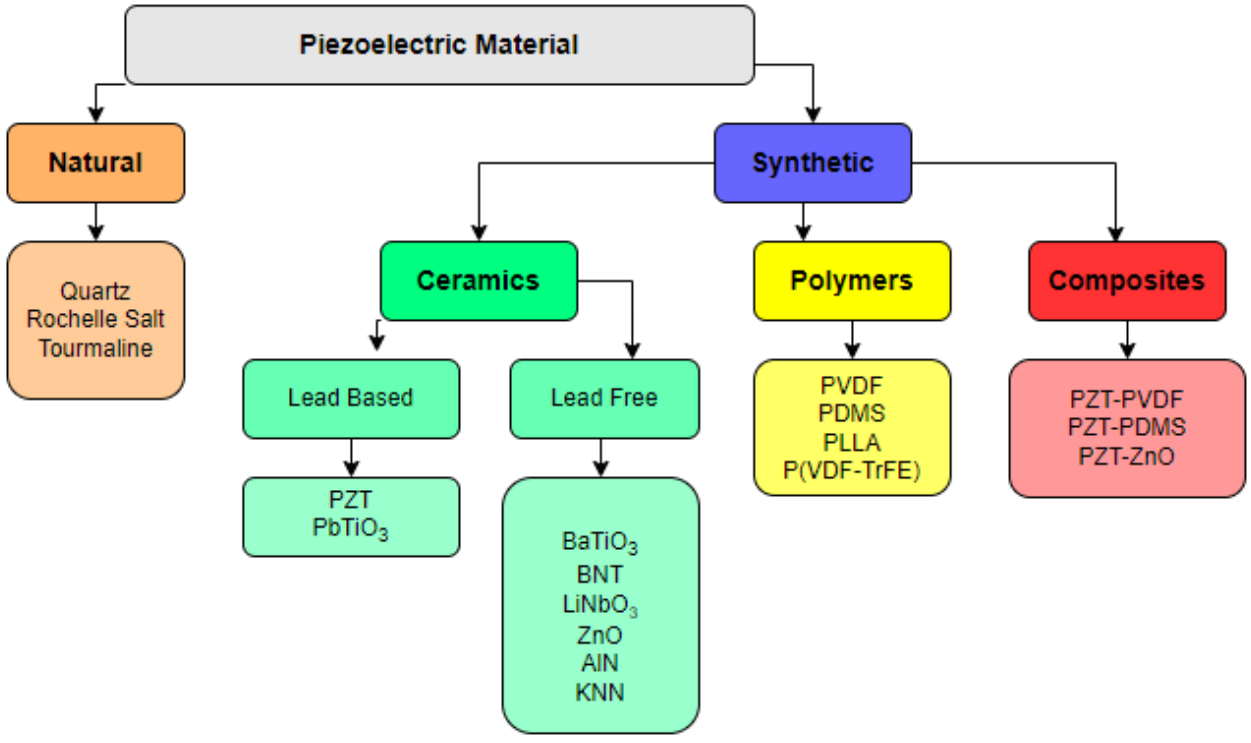

Figure 4. Classification of piezoelectric materials.

2.1. Piezoelectric Ceramics

Piezoelectric ceramics are widely used in various applications due to their excellent piezoelectric properties, robustness, and stability. Piezoelectric materials adopt a variety of crystal structures. First of all, single-crystal and polycrystalline materials can be distinguished from one another. Due to the absence of grain boundaries, the potential to use strongly anisotropic features, and the ability to use non-ferroelectric piezoelectrics, single crystals may exhibit advantages over polycrystalline ceramics. The purity of the starting materials, the growth conditions, and the orientation of the crystals could all influence the quality of single crystals [48]. One of the most well known is quartz [49,50], which has high mechanical quality factors and great electrical resistivity [51,52]. Other single crystals with piezoelectric characteristics include Rochelle Salt [53,54] and lithium niobate ($LiNbO_3$) crystals [55–57]. However, due to their increased cost, lower toughness, and significant damping [58], polycrystalline piezoelectric materials are frequently used. Piezoelectric ceramics are often lead-containing compounds with a perovskite structure [59]. One of the most extensively used and researched piezoelectric ceramic materials is lead zirconate titanate (PZT) [60–65]. Among commercially available piezoelectric materials, PZT is often selected in several applications, because of its high conversion of mechanical energy into electrical energy, being related to its good piezoelectric constant (360 pm/V) [66] and excellent electromechanical coupling coefficient. Because of the material's Curie temperature of 350 °C [67], it can also function safely at high temperatures. PZT, on the other hand, is unsuitable for applications requiring flexibility. Because of its high Young's modulus and density, it is a particularly brittle material. As a result, it has a very high resonance frequency and does not respond effectively to low-frequency ambient vibrations. Pressure sensors, transducers, piezoelectric actuators, and high-power piezoelectric devices are among the many applications for it [68].

Due to the environmental and human health consequences of using lead-based materials [69], research has focused on the development of lead-free piezoelectric materials. Potassium sodium niobate (KNN) [70–72] exhibits a low piezoelectric constant, but its performance can be improved and made closer to that of PZT by modifying its structure through reactive patterned grain growth (RTGG) methods [73–76]. Its goal is to deliver piezoelectric characteristics without the environmental disadvantages associated with lead-based materials.

Ferroelectric materials, such as barium titanate ($BaTiO_3$) [77,78] and bismuth-sodium titanate (Bi,Na)TiO_3, (BNT) [79,80] have not only high saturation polarization but also low residual polarization, allowing for high energy storage density and efficiency to be realized at the same time, which has been a hot spot in dielectric energy storage ceramics research. BNT ceramics have a high Curie temperature (Tc 290 °C) [81], a high temperature stability, and great compatibility with metallic silver electrodes, which offers significant possibilities in the field of dielectric ceramic capacitors. Changes in the domain or grain growth have the potential to improve the characteristics of piezoelectrics [82–85].

Lead-free piezoelectric ceramics include BCZT, which has excellent electrical properties [84], and potassium niobate ($KNbO_3$), which is a ferroelectric perovskite crystal with orthorhombic structure [86] due to strong piezoelectricity [87] and high Curie temperature [88]. $BiFeO_3$ [70] is a perovskite-structured pyroelectric ceramic with a high Curie temperature of roughly 830 °C and theoretically significant spontaneous polarization [89,90]; however, it is not extensively employed due to considerable dielectric losses and weak piezoelectricity [91].

Aluminum nitride (AlN) has greater semiconductor processing compatibility than analogous metal oxide, which is why it is usually used in micro-electromechanical systems devices [92]. Moreover, although having a low piezoelectric constant [93], it possesses a Curie temperature in the order of 1000 °C. Its wurtzite crystal structure facilitates the formation of AlN thin films [94,95]. AlN thin films are ideal for resonators and sensors due to their excellent thermal conductivity and low dielectric and acoustic losses [96].

Lithium niobate ($LiNbO_3$), similar to AlN, is a piezoelectric ceramic material with a low piezoelectric coefficient and a very high Curie temperature [94], and is thus more commonly utilized in high-temperature transducers. It also has a high electromechanical coefficient [97,98], which makes it suitable for usage in resonator MEMS [99]. Lithium tantalate ($LiTaO_3$) [100] and $LiNbO_3$ crystals are industrially manufactured piezoelectric materials that are devoid of rare earths and hazardous components, affordable, and widely employed in the construction of acoustic and optical systems [101]. They are ferroelectric at ambient temperature and, by altering orientations, electrical characteristics such as dielectric constant, pyroelectric coefficient, piezoelectric and electromechanical coupling factor may be increased [102].

ZnO has been one of the most successful materials in recent years due to its ability to optimally transfer mechanical energy into electrical energy at the micro- and nanoscale [103,104]. Zinc oxide has a crystal structure comparable to wurtzite and its piezoelectric capabilities are due to the absence of central symmetry [105]. This piezoceramic has a high tensile strength and can resist massive mechanical deformations for extended periods of time while remaining unaffected by temperature fluctuations [106]. To sinter ZnO, processes such as sputtering [107], pulsed laser deposition [108], spray pyrolysis [109], metal–organic chemical vapor deposition [110], molecular beam epitaxy [111], and 3D printing [112] can be used.

Traditional piezoceramic materials are brittle and stiff. To create more flexible systems, they are frequently produced as thin films, membranes/tapes, or nanowires. In conclusion, because of their capacity to transform mechanical energy into electrical energy and vice versa, they play an important role in many technologies and businesses. Researchers continue to investigate and develop novel materials to increase piezoelectric performance while addressing environmental problems associated with certain lead-containing materials, allowing them to be used in both low- and high-frequency applications.

2.2. Piezoelectric Polymers

Although their light weight and flexibility facilitate excellent deformation and stress absorption, piezoelectric polymers have low mechanical strength and piezoelectric coefficients. They also have low Curie temperatures, which significantly restricts their applicability range. As a result, they are considered as inefficient energy harvesters.

One of the most prevalent piezoelectric polymers is polyvinylidene fluoride (PVDF) [113–115]. It is flexible and has significant piezoelectric capabilities, making it appropriate for a wide range of applications such as wearable devices, sensors, and energy harvesting [116]. It may exist in five different piezoelectric crystalline states. The piezoelectric characteristics of the β phase are superior [117–119].

Siddiqui et al. [120,121] have fabricated a nanocomposite generator based on BT nanoparticles dispersed in polyvinylidene fluoride–trifluoroethylene (PVDF-TrFE) nanofibers prepared through the process of electrospinning. This copolymer is made by combining PVDF with trifluoroethylene, which improves its piezoelectric characteristics and stability. PVDF-TrFE is a material that is frequently utilized in high-performance piezoelectric devices and sensors [122,123]. A piezoelectric copolymer that exhibits a similar phase transition is polyvinylidene fluoride–tetrafluoroethylene PVDF-TeFE [124–127]. Lando and Doll [128] investigated such P(VDF-TeFE) copolymers in 1968, and it is now one of the most extensively used and significant ferroelectric polymers [129,130] because the trans conformation in the copolymers can be stabilized with TeFE units and the crystallinity may approach 90%.

Poly(L-lactic acid) (PLLA), a biodegradable and biocompatible polymer with piezoelectric capabilities, has recently gained popularity [131,132]. While it has lower piezoelectric constants than inorganic piezoelectrics, when in film form, it has a high piezoelectric shear constant. It is ideal for biomedical applications such as tissue engineering and medication delivery systems [133,134]. Zhao et al. [135] investigated the piezoelectric response of cellulose-based electroactive sheets (CEAPs), which are thin cellulose films covered with

metal electrodes. The biodegradability, renewability, and biocompatibility of cellulose-based materials, as well as their intriguing structure and characteristics, contribute to their widespread use in a variety of sectors, including energy harvesting devices, strain sensors, and actuators. They are currently regarded as an important potential material and are being researched by various authors [136–138] because of certain intriguing qualities such as low cost, light weight, biodegradability, and increased production with reduced energy usage. In summary, because they do not include heavy metals, organic piezoelectric materials provide a unique mix of qualities, including flexibility, biocompatibility, and environmental friendliness. They are becoming increasingly crucial in the development of cutting-edge technology, notably in wearable electronics, healthcare, and energy harvesting. To increase piezoelectric performance and broaden the variety of applications, researchers are continually investigating novel organic materials and production methodologies.

2.3. Piezoelectric Composites

Piezoelectric composites are materials composed of a polymer matrix and a piezoelectric ceramic filler in order to obtain specific mechanical and electrical characteristics. These composites are intended to enhance or tailor the performance of piezoelectric materials for a variety of applications. Researchers can produce composites with greater sensitivity, flexibility, or other desirable features by carefully choosing the components and their order. Piezoelectric composites are classified into two types based on the intended material characteristic. Particle-reinforced composites are materials that include piezoelectric particles inserted in a polymer matrix and are used to increase mechanical and electrical qualities. Fiber-reinforced composites, on the other hand, provide stronger mechanical reinforcement and are frequently employed in structural applications [139]. PZT/PVDF [140,141] is a typical example of a piezoelectric polymer–ceramic composite material. Many investigations have found that PZT/PVDF composites exhibit comparable flexibility to native PVDF while having a greater piezoelectric coefficient [142–144]. ZnO-PVDF [145,146] is a great piezoelectric composite because the wurtzite structure of ZnO facilitates the nucleation of PVDF's beta atoms, the polymer's flexibility is paired with the piezoceramic's outstanding piezoelectric characteristics, and it is lead-free. Piezoelectric nanostructures placed on flexible metal substrates have been researched in the realm of implantable or wearable biomedical devices to maximize mechanical, piezoelectric, and biocompatible qualities [147]. The use of nanostructures made up of a vertical array of ZnO nanowires (ZnO NW) [148] inside a polymer matrix of polymethyl methacrylate (PMMA) [149] seems promising [150]. A piezoelectric nanostructure made of ZnO nanowires and the polymer polydimethylsiloxane (PDMS) might accomplish similar results [151]. PDMS is a high-performance elastomer with outstanding optical, electrical, and mechanical capabilities. PDMS is commonly employed in biomedical applications due to its biocompatibility [152,153]. Piezoelectric composites can outperform pure piezoelectric materials in terms of mechanical strength, durability, and flexibility. This makes them suited for applications requiring mechanical strength. Piezoelectric composites' electrical characteristics can be tailored to fit specific needs, such as improved sensitivity, decreased hysteresis, or customized frequency responses. Moreover, they may be tailored to operate under ideal circumstances throughout a larger range of frequency bandwidths. Piezoelectric composites are versatile and customizable, making them useful in a variety of areas such as aerospace, automotive, healthcare, and electronics. Researchers continue to investigate novel composite materials and production processes in order to increase their performance and broaden their uses. Table 1 concludes this section by providing a qualitative comparison of the three groups of piezoelectric materials [47], showing some of the usual values for each group, predicted from a literature survey [3,47,58,154–157]. However, treatments can change those properties.

Table 1. The characteristics of three classes of piezoelectric materials are compared qualitatively.

Property	Ceramics	Polymers	Composites
Piezoelectric Constant (pC/N)	High (100–700)	Low (5–40)	High (50–200)
Electromechanical Coupling Factor	Medium (0.5–0.7)	Low (0.05–0.25)	High (0.4–0.8)
Curie Temperature (°C)	High (150–1000)	Low (−20–100)	Subjective (20–400)
Voltage Constant (10^{-3} Vm/N)	High (10–30)	Low (1–5)	Subjective (1–20)
Flexibility	Low	High	Medium
Density (10^3 kg/m^3)	High (7–8)	Low (1.5–2)	Medium (2–7)
Mechanical Quality Factor	High (500–2000)	Low (3–10)	High (50–1000)
Acoustic Impedance (MRayls)	High (20–30)	Low (1–5)	High (10–20)
Chemical Reactivity	Low	Subjective	Subjective
Feasibility of Manufacturing	High	High	Low
Cost	High	Low	Subjective

3. Piezoelectric Energy Harvester Configuration

The creation of the piezoelectric layer structure is a critical component in the design of piezoelectric energy harvesters. A piezoelectric device that uses a vibrational energy source found in the environment may create as much charge on the structure as it can deform. As a result, the main problem is to build a piezoelectric energy harvester that can produce as much energy as possible across a wide range of stress frequencies while still fulfilling mechanical strength and reliability restrictions. During this phase, the support structure or mounting mechanism must be designed to guarantee that the piezoelectric material may flex or deform in response to vibration or mechanical stress. The mechanical interaction between the vibration source and the piezoelectric material should be optimized in the design. The limits imposed by the application and the piezoelectric material in question should be addressed in the design, since the material's production procedures impose non-negligible dimensional constraints. Structures can be classified into four main categories:

- Cantilever beam;
- Circular diaphragm;
- Cymbal transducer;
- Stacked array type.

3.1. Cantilever Beam

In most applications, cantilever-type piezoelectric energy harvesters are the most common. The structure with one end embedded and the other free promotes the generation of enormous strains during the excitation of the structure on the limited base. Cantilever beams can be unimorphic or bimorphic, depending on the number of piezoelectric layers linked to the support structure. A piezoelectric foil plus a layer of metallic substance make up the unimorph kind. The bimorph, on the other hand, has a center layer of metal material connected to two layers of piezoelectric material on the top and bottom surfaces. Flexural excitation is chosen in the cantilever beam form since multiple publications demonstrate that the matching "mode 31" piezoelectric connection gives the highest energy conversion efficiency [158,159]. In addition, as illustrated in Figure 5, an extra mass can be supplied to the free end of the cantilever beam to enhance deformation and tune its resonance frequency with regard to the available vibration source [160,161].

Substantial contributions to the development of optimal piezoelectric devices that use vibrational energy have been recognized in the literature [45,162–169]. A cantilever beam has several advantages, including low resonance frequencies, high average strain for a given input force, and the ability to be easily generated through a microfabrication process due to its simple form. Yet, a broader study of various design configurations can increase the energy harvesting device's performance [170,171]. Its functioning concept is based on producing a state of deformation inside the beam, the distribution of which is referred to as butterfly in a general section. It is positive on one side of the tension fiber and negative on the other, fluctuating linearly between these extremes and canceling out

on the neutral axis. The bending moment and consequent normal stress in the traditional rectangular scavenger diminish linearly from the fixed end to the free end [172].

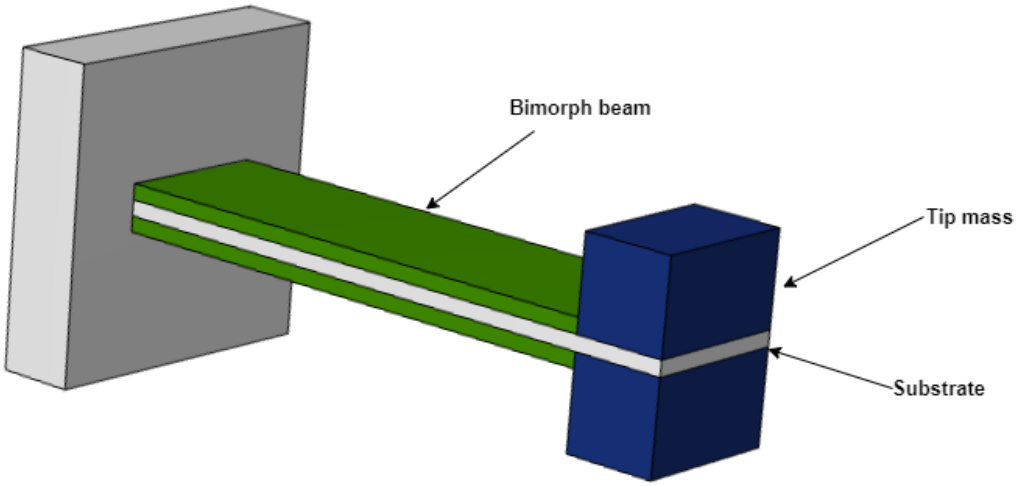

Figure 5. Layout of a common piezoelectric vibration energy harvester.

According to the uniform strength criterion, a rectangular-plan cantilever beam has a maximum stress strain in the embedment that decreases linearly along the length until it cancels out at the free tip, in contrast to a triangular-plan cantilever beam, which allows for uniform stress distribution along the beam surface. Nevertheless, due to technological limits for production and the area necessary to connect the test mass, the trapezoidal-plan cantilever beam is used as a compromise. This theory is congruent with the application at hand in that it permits the material to retain as much elastic potential energy as feasible. Many studies have been based on this configuration, including [61,173,174]. Roundy et al. [173] present research on piezoelectric energy harvesting designs capable of optimizing power production, as shown in Figure 6.

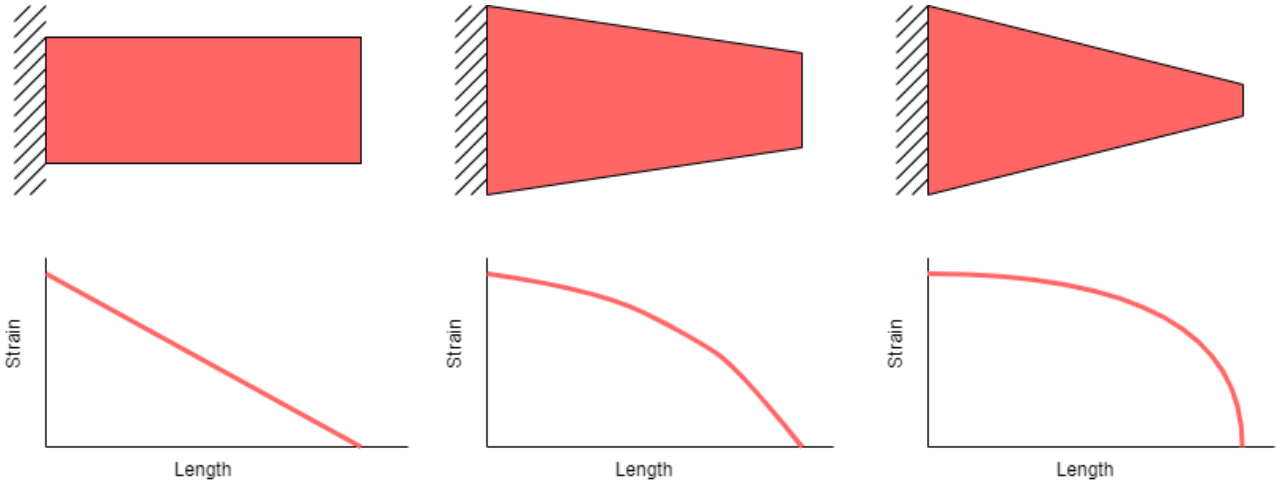

Figure 6. Rectangular and trapezoidal beam comparison.

Figure 7 by Benasciutti et al. [173,174] shows a unique option provided by an inverted trapezoidal construction. When the two constructions, direct trapezoidal and inverse trapezoidal, are compared, the latter greatly increases the stress at the interlock and offers a greater area at the free end, making placing of the test mass easier.

Mantova et al. [175] investigate the effect of length-to-width ratio on piezoelectric cantilever beams. Long thin beams with a length-to-width ratio greater than one demonstrated the predicted increase in power output when the beam was tapered. In contrast, short

broad beams with a length-to-width ratio of 1 indicated a drop in power output when the beam was tapered. Tapering resulted in a more equal stress distribution along the beam surface's centerline. Tapering has a favorable influence on the mechanical and piezoelectric performance (power) of piezoelectric cantilever binders only if the device beams are long and thin, according to this construction analysis.

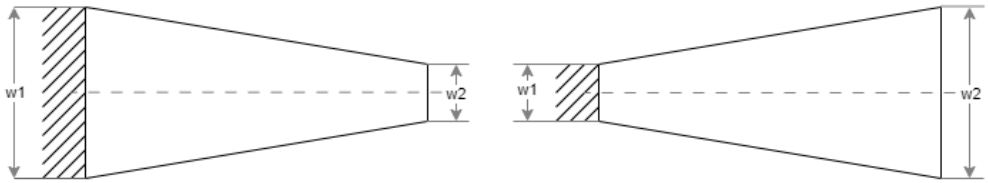

Figure 7. Direct and reverse trapezoidal cantilever.

Gogoi et al. [176] use a mathematical method to compare the rectangular plan, trapezoidal plan, and T-model, and evaluate the influence of geometrical parameters on the structure's electrical output performance.

3.2. Circular Diaphragm

A diaphragm is a thin membrane, constructed of a piezoelectric layer, that is used to detect or create sound waves, pressure, or strain. It is made up of a thin piezoelectric disk that is put on a metal plate that is greater in diameter than the piezoelectric disk, Figure 8. A test mass is connected to the middle of the diaphragm to boost power output and intensify performance during low-frequency operation [177]. Piezoelectric diaphragms are commonly found in microphones, loudspeakers, pressure sensors, force transducers, and vibration detecting devices. They are regarded for their sensitivity, ability to work throughout a wide frequency range, and quick reaction capabilities [178].

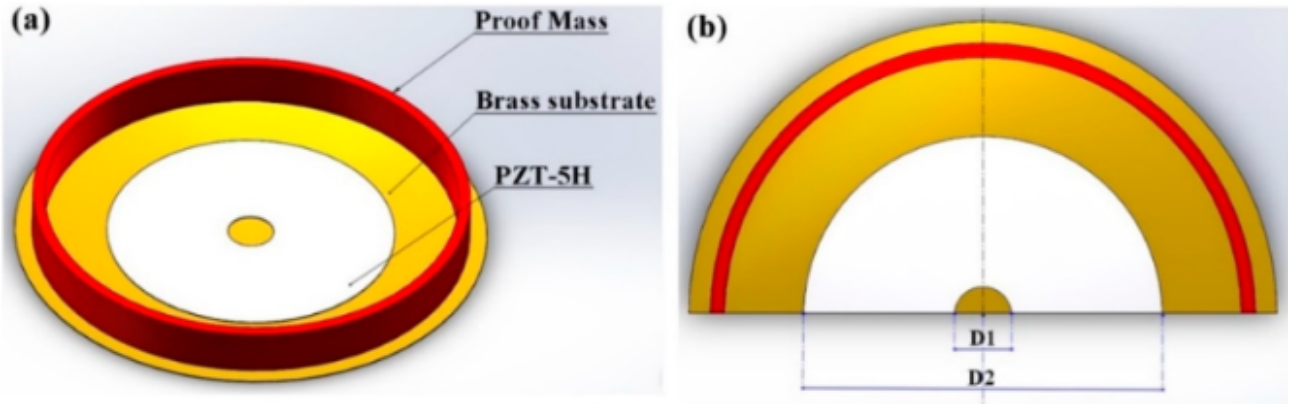

Figure 8. Schematic (**a**) and parametric (**b**) structure of piezoelectric circular diaphragm [177].

3.3. Cymbal Transducer

Cymbal transducers, which are effective in situations requiring larger impact pressures, are made up of a piezoelectric layer sandwiched between two metal terminal caps on either side. When an axial stress is applied to the metal terminal caps, it is amplified and turned into a radial stress, resulting in a larger piezoelectric coefficient and, as a result, more charge production by the piezoelectric energy harvester [179]. The plate structure proposed by Newnham et al. [180] is one example. It is made up of two plate-shaped metal end caps with a piezoelectric disk sandwiched between them, as seen in Figure 9. The plate-shaped metal end caps increase the piezoelectric disk's strength under heavy loads. The metal end caps function as a mechanical transformer due to the existence of a cavity [181].

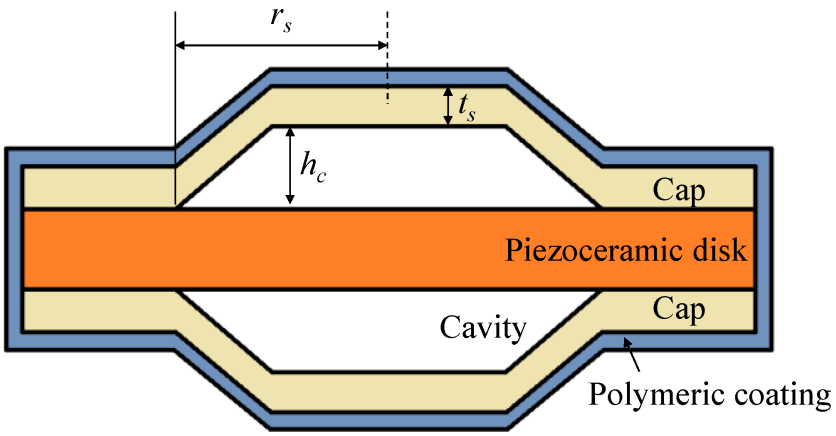

Figure 9. Schematic structure of piezoelectric cymbal transducer [182].

Piezoelectric cymbal transducers are the most widely accessible commercially and may be simply mounted on any flat surface using an adhesive. As a result, several research publications have concentrated on this sort of element in piezoelectric tiles [183–185].

3.4. Stacked and Array Structures

Designed for high-pressure applications, piezoelectric stack transducers are made up of several layers of piezoelectric material layered on top of one another with their polarization directions matching the applied force. A piezoelectric array is a grouping of piezoelectric devices that are placed in an array or in a precise sequence for sensing, signal production, or other uses. Piezoelectric arrays are utilized to take advantage of the piezoelectric capabilities of materials in a range of applications, ranging from medical imaging to ultrasound to active vibration reduction in structures. Piezoelectric arrays are essential components of ultrasonic imaging equipment. In this case, the array's piezoelectric components create ultrasonic pulses that are transferred into the human body. As ultrasonic pulses bounce off inside tissues, the same piezoelectric devices detect the wave's return and provide a real-time picture.

Chen et al. [186] give a demonstration of an annular piezoelectric array composed of several concentric elements, fabricated by MIP-SL (Mask-Image-Projection-based Stereolithography) technology. The array obtained by printing exhibits stable piezoelectric and dielectric properties. Compared with a conventional single-element ultrasonic transducer, the printed-matrix ultrasonic transducer successfully changes the shape of the acoustic beam and leads to a significant improvement in spatial resolution. In order to optimize the voltage output/electric charge, piezoelectric stacks are utilized [187–190]. In Cascetta et al. [191], arrays constructed of PZT diaphragm stacks under the top plate were employed to boost the power provided for piezoelectric energy harvesting. To accommodate for deformation, nine piezoelectric diaphragm stacks were employed, each consisting of five piezoelectric diaphragms separated by a ring. The design of a piezoelectric array will thus be determined by the application's unique sensing or signal generating requirements. Piezoelectric arrays can be used to monitor pressure and detect changes in force distribution on a surface in applications such as vehicle tires or laboratory pressure measurements.

3.5. Other Innovative Configurations

Innovative architectures that increase the efficiency of piezoelectric energy harvesters while maintaining a configuration consistent with the respective field of application have been investigated in the literature over the years.

Ansary et al. [192] suggest fan-folded piezoelectric energy harvesters for powering pacemakers, which comprise bimorph piezoelectric beams folded on top of each other. They demonstrated experimentally that the fan-folded design (shown in Figure 10) may

be utilized to lower the high inherent frequency of tiny devices employed in energy harvesting applications.

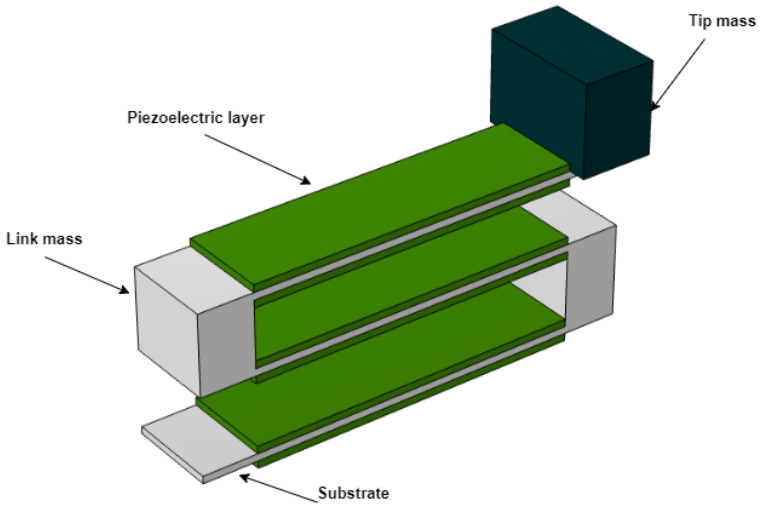

Figure 10. Schematic structure of fan-folded piezoelectric energy harvesters.

Dong et al. propose a piezoelectric spiral energy harvester appropriate for vibrational energy sources in [193,194]. The spiral construction, which is cantilevered at various locations along its circumference, is intended for compactness, low resonance frequency, and low damping coefficient, Figure 11. This option increases compliance in a restricted location by maximizing the length of the cantilever arm. The primary goal of this design is to magnify the input mechanical energy, the transducer of which is the cantilever beam to which this spiral is coupled, considerably increasing the device's diameter.

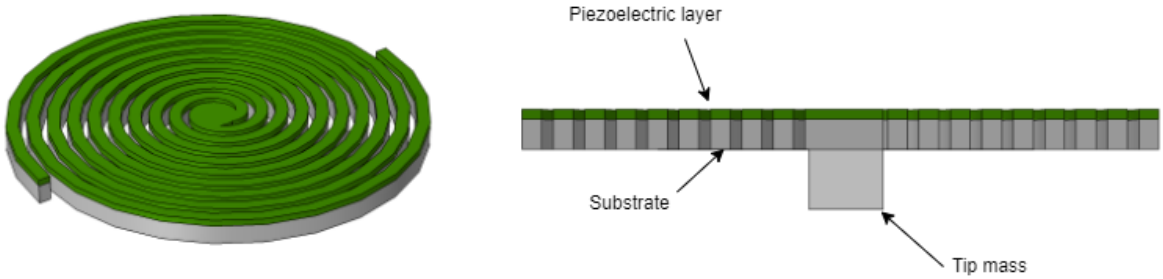

Figure 11. Schematic structure of spiral piezoelectric energy harvesters.

It is crucial to note, however, that this geometry poses some substantial obstacles. One of the most challenging issues is the fabrication stage, which is particularly problematic for single-arm spirals due to residual tensions during the material deposition process, which can cause bending and cracks in the spiral. Moreover, the complexities of electrical charge distribution on spirals need more sophisticated electrode designs. They discovered that the output power is affected by the frequency and direction of the external force, as well as the resistance load.

Castagnetti et al. [195] present an innovative design that makes use of dynamic magnification. It entails attaching the structure to an intermediary spring–mass system that is connected to the vibrating base structure. As a result, the ambient energy that stimulates the structure will intensify the dynamic response and, as a result, enhance the energy provided. This approach is utilized in a number of literary works [196–200]. Figure 12 depicts Castagnetti's proposed structure, which is inspired by fractals with dynamic magnification.

Dong et al. described an in vivo cardiac energy harvesting technique that eliminates contact of the harvesting device with the heart and interference with cardiovascular function [201]. To transfer mechanical energy from the lead of an implantation pacemaker

or defibrillator into electrical energy, a piezoelectric energy harvesting device based on a porous thin film with a self-enveloping helical shape was created. Figure 13 shows the similar configuration studied by [202].

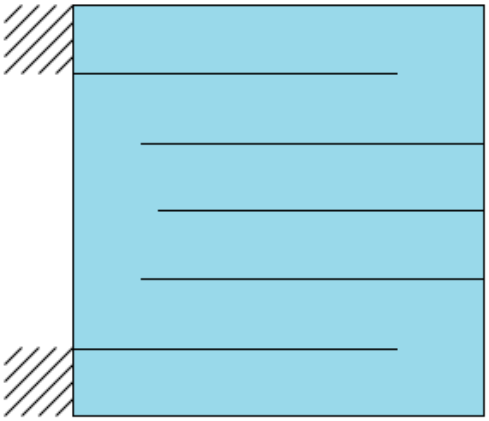

Figure 12. Structure of fractal geometry with dynamic magnification.

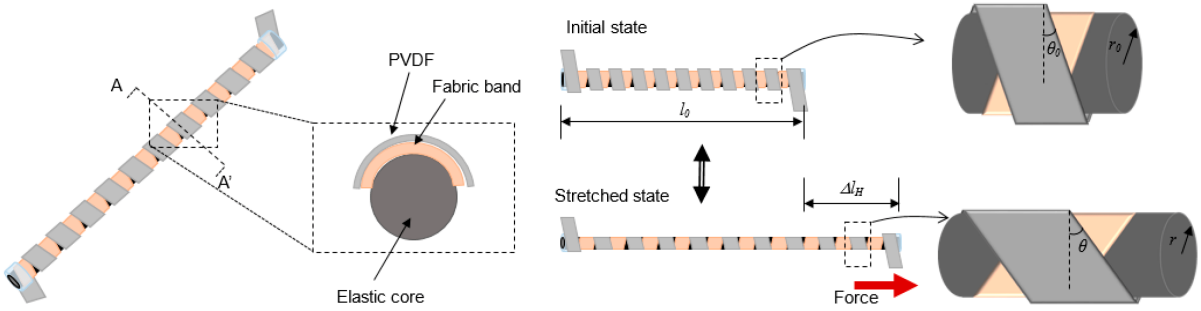

(**a**) (**b**)

Figure 13. (**a**) Schematic structure of helical piezoelectric energy harvester and (**b**) when a stretching force is applied to it [202].

Table 2 summarizes the advantages and disadvantages of the four basic types of configurations for piezoelectric structures.

Table 2. Advantages and disadvantages of piezoelectric energy harvester configurations [44].

Type of Configuration	Advantages	Disadvantages
Cantilever beam	Simple structure Low fabrication cost Lower resonance frequency Power output is proportional to proof mass High mechanical quality factor	Inability to resist a high impact force
Circular diaphragm	Compatible with pressure mode operation	Stiffer than a cantilever of the same size Higher resonance frequencies
Cymbal transducer	High energy output Withstands high impact force	Limited to applications demanding high magnitude vibration sources
Stacked and array structures	Suitable for pressure mode operation Higher output from d_{33} mode	High stiffness

4. Piezoelectric Harvesting Circuits

A typical piezoelectric generator is represented by an equivalent electromechanical model, shown in Figure 14.

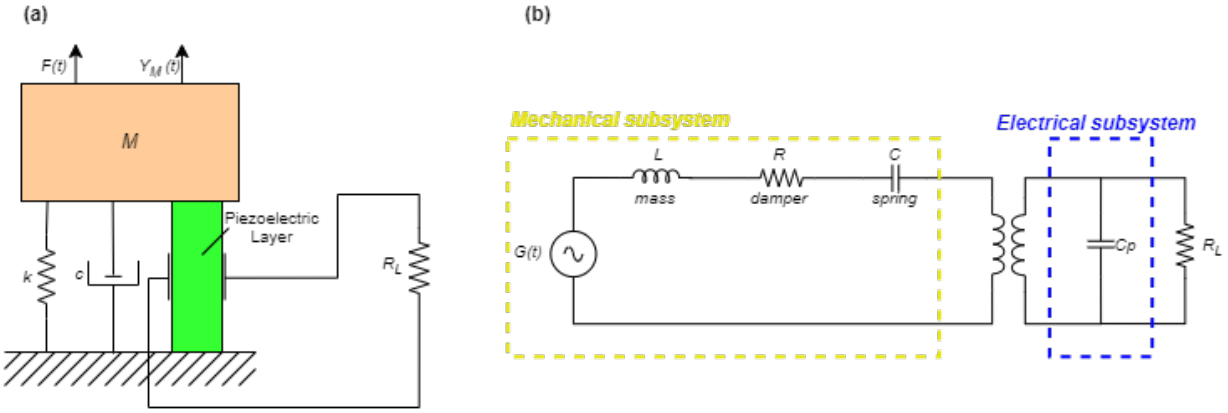

Figure 14. (**a**) Electromechanical model of the piezoelectric vibration energy scavenger. (**b**) Equivalent circuit model of the bimorph vibration energy scavenger.

This circuit includes the following:

- The source G(t): expressed in the mechanical domain by the input vibration intensity;
- The inductor L: expressed in the mechanical domain by the equivalent inertial mass;
- The resistor R: expressed in the mechanical domain by the damping of the material composing the piezoelectric generator and other mechanical losses;
- The capacitor C: expressed in the mechanical domain by the elastic energy of the transducer;
- The capacitor Cp: the value of electrical capacitance measured between the two electrodes of the piezoelectric element.

The circuit shown in Figure 14 in electronic integrated circuits is simplified with an AC current generator connected in parallel to the piezoelectric's capacitance Cp and internal resistance Rp.

To optimize energy management and power the load, the piezoelectric energy harvested from the device must be rectified, stored, and conditioned according to the application. This section describes the most appropriate interfaces for this technology, such as standard energy harvesting circuits, also known as full-bridge rectifiers (FBRs), synchronized harvesting circuits on inductors (SSHIs), synchronous electric charge extraction (SECE), and the pulsed synchronous charge extractor (PSCE) interface circuit, which is based on the integrated design of complementary metal oxide semiconductors (CMOSs).

4.1. Standard Energy Harvesting Circuit

As explained in the introduction, a piezoelectric device subjected to an external mechanical force develops a stress/deformation condition on the structure, which generates an electric field and develops a charge on the terminals owing to the direct piezoelectric effect. This electric energy can be made up of positive or negative signals and must be rectified before it can be used by an outside user. As a result, an interface circuit is required to convert the AC current from the piezoelectric generator to DC power using an AC/DC converter. A standard energy harvesting circuit is a basic design used to capture and convert energy from various environmental sources such as solar radiation, vibration, thermal gradients, or radio frequency (RF) signals into usable electrical energy. Energy harvesting circuits are often built to be versatile and adaptable to a variety of energy sources and applications. Particular components and their arrangement may differ based on criteria such as energy source type, required output voltage and current, and efficiency requirements.

The standard single-stage energy harvesting circuit, illustrated in Figure 15, consists of a full-bridge rectifier and permits AC-to-DC conversion in the simplest method possible. It also has high stability when compared to other rectifiers.

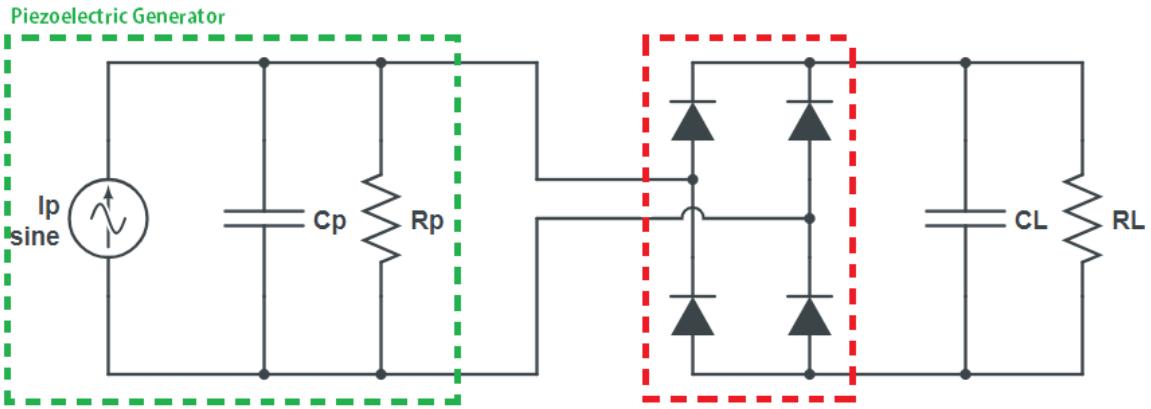

Figure 15. The standard full-bridge rectifier (FBR) circuit.

A rectifier bridge, also known as a diode bridge, is a component that prevents the charge from moving backward from the circuit to the piezoelectric layer and rectifies the current. Every pulse may store energy, independent of charge sign, which can be both positive and negative. This sine wave rectifier speeds up charging of the linked capacity. Otherwise, when crossed by alternating current, the diode would only pass the positive half-wave and block the negative half-wave. It does, however, have a significant disadvantage in that its conversion efficiency is low due to the impossibility of impedance matching and the diode's direct voltage drop, resulting in a large conduction loss and, as a result, a reduction in the energy extracted by the piezoelectric generator. Asis et al. [203] developed an active AC–DC full-bridge rectifier with a high-performance metal oxide semiconductor field-effect transistor (MOSFET) with PEH switching control in their research. Studies conducted by Le et al. [204] compare different passive and active half-wave and full-wave rectifiers in terms of efficiency and output power. They confirm the thesis that half-wave rectifiers are relatively inefficient because they only employ half of the input AC cycle, squandering the other half.

Sometimes, the energy delivered by a single event is insufficient to power a sensor or many electronic devices require a continuous and constant current to function properly. On the other hand, when energized, energy harvesters produce an unprocessed AC-type current that must be rectified and then stored in a temporary capacitance before being delivered to the user. As a result, an intermediary step consisting of a DC/DC converter is added downstream of the rectifier bridge to prevent a fast discharge of the battery or even saturation of the charges being stored. This mechanism regulates and adapts the temporary capacity's output voltage. Figure 16 depicts a generalized design for two-stage energy harvesting [205].

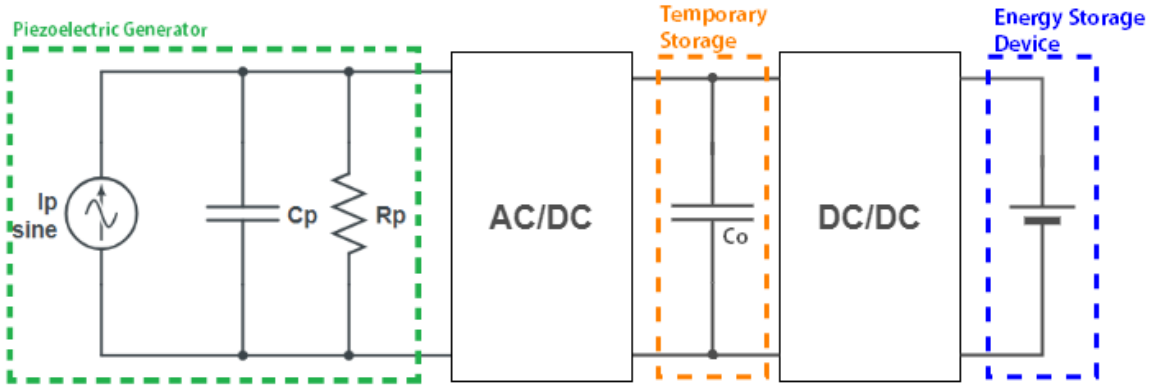

Figure 16. Generalized two-stage energy harvesting circuits.

4.2. Synchronized Switch Harvesting on Inductor (SSHI)

The models presented thus far improve the voltage drop across the rectifier bridge diode but have no effect on the impedance matching problem. Guymar et al. [206] extended the Synchronized Switch Damping (SSD) technique of Richard et al. [207] by introducing a biased rectifier dubbed Synchronized Switch Harvesting on Inductor (SSHI). They discovered that, depending on the electromechanical coupling in the system, the collected power may be enhanced (relative to the usual AC–DC conversion method) by 250 to 900% [208,209]. SSHI is a sophisticated energy harvesting technology that captures and converts energy from sources with intermittent or low-frequency vibrations, such as those present in the environment or mechanical systems. SSHI works on the notion of energy harvesting by employing synchronized switching mechanisms on an inductor and a capacitive device. It maximizes energy extraction by making use of the periodic nature of environmental vibrations or mechanical oscillations. An inductor and a switch are critical components in converting the FBR circuit to the SSHI circuit. It stores and transmits energy by generating electromagnetic fields when a current runs through it. SSHI employs a switching circuit that connects and disconnects an inductor from a storage capacitor on a regular basis. To improve energy transmission, the switching is synced with the frequency of mechanical vibration or oscillation. Negative power is created in the basic AC–DC power harvesting circuit (Figure 15) because the output current and generated voltage cannot keep the same phase; this implies that some of the captured power may return to the mechanical portion, resulting in a loss of harvested power [210]. The SSHI circuit addresses this issue by including a switch route. As the capacitor voltage hits a maximum in the opposite polarity, the switch opens instantly, causing the capacitor voltage to reverse. This permits the capacitor charge to be collected rather than discharged into the waste [211]. Synchronization guarantees that energy is caught at the ideal position in the vibration cycle, enhancing energy transfer efficiency.

SSHI circuits can be configured in two ways: in series (Figure 17) and in parallel (Figure 18). The only variable is whether the switch route is linked in series or parallel with the rectifier [212]. Lallart and Guyomar [213] created a self-powered SSHI interface that can conduct switching operations automatically whenever the output voltage reaches its maximum.

The typical SSHI circuit has significant start-up issues, limiting its performance in low-amplitude and variable-amplitude vibration settings. Du et al. [214] suggest a novel structure with an SSHI starting circuit that addresses the startup issue by restricting SSHI rectifiers. The starting circuit can be used to monitor the SSHI circuit's working state and restart the SSHI circuit in the event of unpredictable functioning. The suggested circuit, when compared to the traditional SSHI rectifier, may greatly lower the minimum input excitation amplitude before power extraction and extend the power extraction interval. Moreover, the standard SSHI circuit's limited operational bandwidth and low harvesting capacity limit the performance of the PEH system. In summary, Synchronized Switch Harvesting on Inductor is a sophisticated energy harvesting system that successfully absorbs energy from intermittent or low-frequency vibrations through the use of synchronized switching mechanisms. It has benefits in terms of efficiency and versatility, making it appropriate for a wide range of applications requiring energy harvesting from environmental sources. It does, however, contain architectural challenges that must be addressed for successful implementation, as precise synchronization and control methods are required. In order to maintain efficiency, the switching frequency of the circuit must be calibrated with the frequency of mechanical vibration or oscillation. Lastly, the selection of the electronic components that comprise the interface circuit, particularly the inductor and capacitors, is critical for optimizing performance.

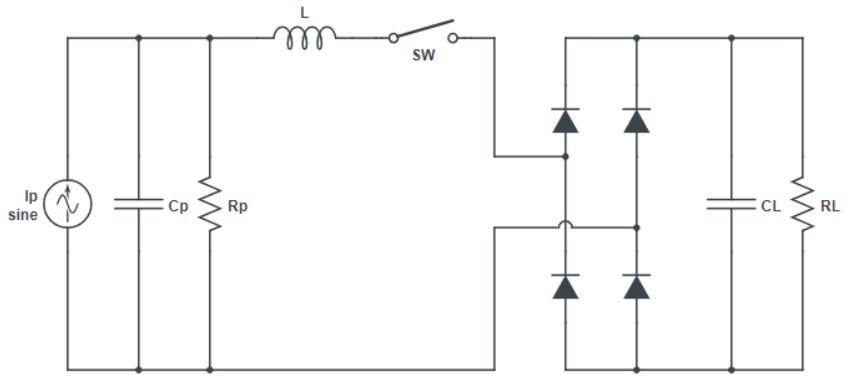

Figure 17. S-SSHI energy harvesting circuit.

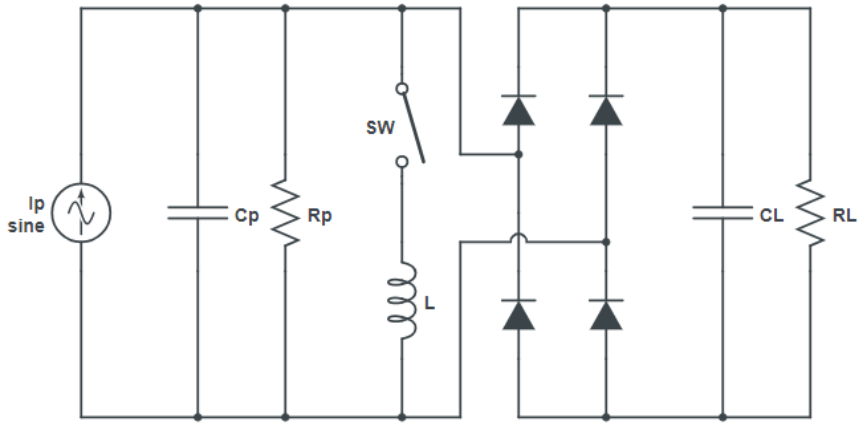

Figure 18. P-SSHI energy harvesting circuit.

4.3. Synchronous Electrical Charge Extraction (SECE)

Synchronous Electrical Charge Extraction, like the SSHI circuits, uses an inductor and a switch (SECE). The SECE circuit, unlike the SSHI circuit, does not have a load dependence, which improves the efficiency of the energy extracted. This enables it to be used successfully to gather broadband energy under random vibration settings. Because of these benefits, it has become one of the most often used energy management circuits for piezoelectric energy harvester systems. The SECE circuit, initially developed by Lefeuvre et al. [215], employs an LC resonant circuit to first transport the energy stored in the piezoelectric capacitor to the inductor and then to the load through a DC–DC converter. With this method, the power extracted does not depend on the load; therefore, the load can vary without affecting the efficiency. Figure 19 depicts the wiring schematic for the SECE interface circuit.

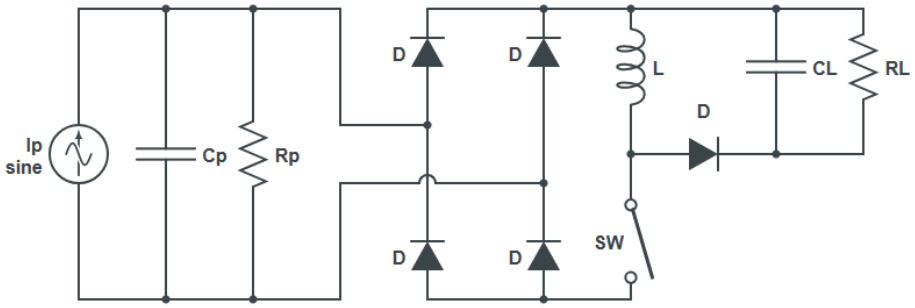

Figure 19. SECE energy harvesting circuit.

Cai et al. [216], demonstrated a way for increasing bandwidth in the classic SECE system by inserting two time delays. The circuit changes these time delays adaptively for maximal power production at out-of-resonance frequencies. The bandwidth is raised by 71% while the power consumption of the circuit remains low at 0.85 W. Synchronous electric charge extraction is a method used in energy harvesting, specifically for extracting electric energy from piezoelectric materials. It is a way for boosting the overall efficiency of energy conversion by maximizing charge extraction from piezoelectric devices. The primary idea behind SECE is to optimize the energy harvesting process by synchronizing the extraction of electrical charge from piezoelectric material with its mechanical deformation or vibration. SECE enhances the effectiveness of mechanical vibration or deformation to electrical energy conversion, resulting in improved total energy harvesting efficiency. SECE further guarantees that energy is gathered at the most appropriate periods in the vibration cycle by coordinating charge extraction with mechanical deformation. When compared to non-synchronized approaches, this circuit can result in a large increase in the quantity of electrical energy gathered by piezoelectric materials. When the electromechanical coupling coefficient is large, however, the SECE technology performs poorly because the SECE circuit collects too much energy, unduly dampening the mechanical resonator, breaching the initial fitting condition, and decreasing the ultimate energy harvesting efficiency. Leuvre et al. [217] suggest a change to the classic SECE circuit, providing a novel phase-shift SECE interface (PS-SECE). This circuit enhances the frequency bandwidth and increases the maximum cumulative power in systems with high coupling. There are critical areas where additional care is required to maintain optimal circuit efficiency. To begin, perfect timing and synchronization are required to match the mechanical strain or vibration frequency, which might be difficult. As with the SSHI circuit, component selection, including switching elements and energy storage components, is critical to optimizing the SECE system's performance. SECE can power low-power sensors in wireless sensor networks without the need for external power sources or frequent battery changes. It can absorb energy from vibrations in infrastructure and offer a constant power supply for monitoring devices in structural health monitoring. Shareef et al. [218] offer a novel arrangement without a rectifier. They suggest an SECE technology with a bidirectional switch to perform AC–DC conversion; the inductor is only switched on for a brief duration when the PEH system's output voltage peaks and numerous inverters can share an inductor. Wang et al. [219] introduce a high-precision active peak detector to control the switch in the SECE circuit, which is driven by a thermoelectric generator circuit and consumes little power. This circuit not only eliminates the usual rectifier bridge construction and delivers steady DC voltage, but it also increases the energy harvesting efficiency of PEH by around 41.9 percent.

4.4. Pulsed Synchronous Charge Extractor (PSCE)

To reach acceptable efficiency at the break of losses on the diodes, SSHI and SECE circuits require the employment of piezoelectric energy harvesters capable of producing several milliwatts of electricity [220]. This difficulty is alleviated by CMOS devices, which lack a full-wave rectifier, albeit at the penalty of inefficiency [221]. Kwon et al. [222] presented a CMOS that, although allowing applications with PEHs producing low voltages, lacks passive starter, restricting its practical applicability. The completely autonomous PSCE (pulsed synchronous charge extractor) chip [223] overcomes some of the constraints. PSCE is a technique that improves conversion efficiency and reduces power losses caused by parasitic series resistors. It is based on the SECE technology. To summarize, because the SECE technique's key feature is to transfer power in a very small time frame relative to the excitation period, the current that happens during this brief term can easily reach values of many tens of milliamps for a total transmitted power of a few milliwatts. Resistors introduced to the current route as parasitic components can cause large power losses, lowering power harvesting efficiency [224]. The functional diagrams of the PSCE interface, which comprise an NVC, three switches, and an inductor, are shown in Figure 20. The NVC "rectifies" the piezoelectric voltage; however, it is not a genuine rectifier because it

cannot stop reverse current. The switches are set appropriately to allow the inductor to temporarily store the energy collected from the piezoelectric harvester during the transfer procedure. This energy is subsequently released to the storage capacitor and dissipated via the load.

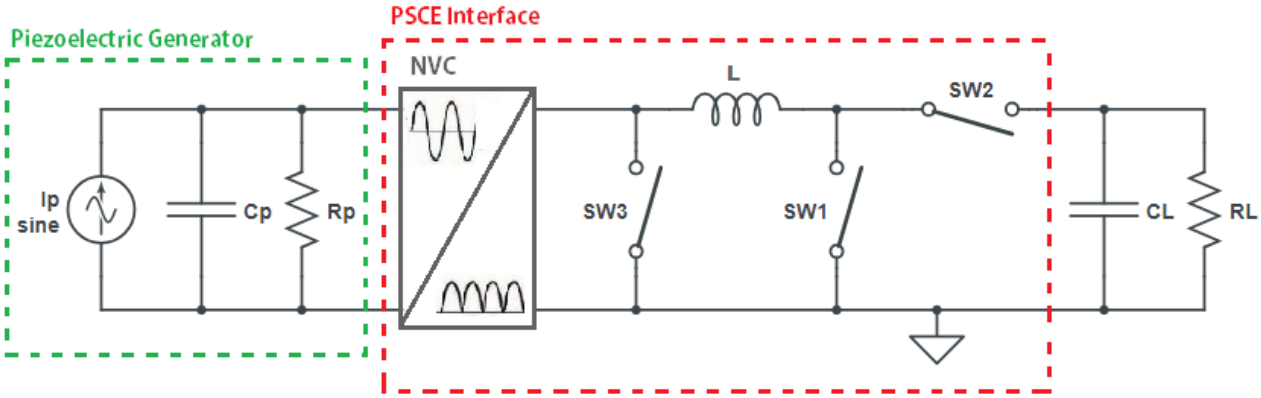

Figure 20. PSCE energy harvesting circuit.

The low-power device is adaptable and may be utilized in a wide range of PEH frequencies, PEH voltages, and buffer voltages, making it useful in a number of circumstances. As compared to a passive full-wave rectifier with a modest voltage drop, this chip dramatically increases the power extracted. Also, the chip can start even if the buffer capacitor is drained; the buffer capacitor is passively charged by bypass until the minimum supply voltage is met. A pulsed synchronous charge extractor is a specialized circuit or device used in energy harvesting applications, especially those involving piezoelectric materials. PSCE is intended to optimize electrical charge extraction from piezoelectric devices in a synchronous pulsed manner, hence maximizing energy harvesting efficiency.

5. Energy Harvesting Technology Applications

Table 3 highlights efforts to offer the most essential information for comparing different transducer types, sizes, and output powers of different piezoelectric binders; more details of each study may be obtained in the related articles.

Table 3. Generator output performance based on various piezoelectric materials.

Device Description	Dimensions	Output Performance	Ref.
Cantilever beam in PZT-5H	$60 \times 31 \times 0.2$ mm^3	The peak output voltage is 18 V, and the electric power is 29 mW under excitation force 1 g and frequency 26.6 Hz.	[225]
PZT thin film on buffer-layer with $PbTiO_3$ inter-layer	$800 \times 100 \times 10$ μm^3	From a vibration of 0.39 g acceleration at its resonance frequency of 528 Hz, the built energy harvester generated 1.1 μW of electrical power with 4.4 V peak output voltage.	[226]
ZnO NW and a dielectric PE film on a wearable textile substrate	10 cm^2	When activated by acoustic vibrations at 100 dB, the open-circuit voltage is 8 V and the short-circuit current density is 0.15 μA/cm^2.	[227]
AlN-based piezoelectric devices	$1.01 \times 5.0 \times 5.0$ mm	At 2.0 g acceleration and 572 Hz resonant frequency, the maximum output power is 60 μW.	[228]

Table 3. *Cont.*

Device Description	Dimensions	Output Performance	Ref.
P(VDF-TrFE) thin film	0.09 cm^2	Nanogenerator has up to 7 V open-circuit voltage and 58 nA short-circuit current with a current density of 0.56 $\mu A/cm^2$.	[229]
Electrospun PVDF/$BaTiO_3$ nanogenerator	2 cm × 6 cm × 50 μm	At the resonance frequency of 15.7 Hz, the highest piezoelectric output power was 0.243 W (15 wt% PVDF and 5 wt% $BaTiO_3$), acetone/DMF (6:4 vol./vol.) under 10 M*W*.	[230]
Sea-sponge-inspired BCZT		When compressed by 12%, the output voltage is 25 V, the current density is 550 nA/cm^2, and the power density is 2.6 mW/cm^2.	[231]
PLLA nanofibers		With a strain deformation angle of 28.9°, the open-circuit voltage is 0.55 V and the short-circuit current is 230 pA. The maximum electric power produced by human joint motion is 19.5 nW.	[232]
Cellulose nanofibers/PDMS		The open-circuit voltage is 60.2 V, the short-circuit current is 10.1 A, and the power density is 6.3 mW/cm^3 when the oscillator is excited at 10 Hz.	[233]

6. Conclusions

Piezoelectric energy harvesting is a candidate technological approach for generating electricity from renewable sources. Its tremendous potential has been proved in a variety of applications, ranging from energy harvesting from vibration to wearable devices. New applications like charging portable electronic devices and low-power sensors are gaining popularity quickly. These applications have the potential to significantly affect daily living and energy efficiency. Advanced piezoelectric material research has cleared the road for more efficient and lightweight electronics. The utilization of versatile and novel materials has the potential to transform the industry. Although PZT is the most common and has the best piezoelectric coefficients, lead toxicity limits its use today. A survey of the literature provides an overview of piezoelectric materials known to date. Piezoelectric composites made of polymer matrix and piezoceramic materials may be a promising material since the proper quality compromise may be reached depending on the composition. Piezoelectric device design and optimization remain key issues. Little changes in design can result in considerable benefits in efficiency and overall performance, according to research. After the classification of the four types of layouts that predominate in the world of energy harvesters, new configurations popular in the medical field that give the structure lightweight flexibility and operate well at low frequencies are explained. Despite substantial advances, there are still obstacles to overcome, including effective integration with other energy sources and appropriate energy management. This study discusses the energy delivery interfaces provided by terminals put on the surface of piezoelectric materials. A piezoelectric energy collector often includes an AC–DC converter, a two-stage conversion circuit, or employs nonlinear methods like SSHI, SECE, or PSCE. Although piezoelectric materials have gone a long way since their discovery, material characteristics still have a lot of space for development in order to enable new applications. Today's electronics development trend is to minimize device size, reduce power consumption, and increase device flexibility and integration capabilities. Piezoelectric materials are progressing toward being lead-free and having a high voltage coefficient. Many research organizations are focusing on innovative green manufacturing methods such as additive manufacturing, while others are investigating biodegradable piezoelectric materials. PEHs' bandwidth is projected to be expanded for a wide range of non-fixed external frequencies. This suggests that using a nonlinear

structure to utilize the internal resonance of structures is a superior option for increasing conversion efficiency. To get the most power out of the PEH, the interface circuit must be properly constructed to accomplish impedance matching. Currently, the development trend in electronics is to lower device size and power consumption, and increase device flexibility and integration capabilities. Therefore, piezoelectric energy harvesters offer a number of beneficial perspectives to increase energy efficiency and to promote sustainable applications. Interdisciplinarity and collaboration among scientists, engineers, and designers are required to realize this technology's full potential. In the future, the sector will expand, leading to novel solutions to global energy concerns.

Author Contributions: Conceptualization, A.C., E.B. and C.D.; methodology, E.B.; validation, A.C.; formal analysis, C.D.; investigation, A.C.; data curation, A.C.; writing—original draft preparation, A.C. and C.D.; writing—review and editing, E.B. and C.D.; visualization, A.C.; supervision, E.B. and C.D.; project administration, E.B. and C.D.; funding acquisition, E.B. and C.D. All authors have read and agreed to the published version of the manuscript.

Funding: This research was funded by FSE REACT-EU Azione IV.5 "Dottorati su tematiche Green" of D.M. 1061/2021.

Data Availability Statement: Not applicable.

Conflicts of Interest: The authors declare no conflict of interest.

References

1. Shirvanimoghaddam, M.; Shirvanimoghaddam, K.; Abolhasani, M.M.; Farhangi, M.; Barsari, V.Z.; Liu, H.; Dohler, M.; Naebe, M. Towards a Green and Self-Powered Internet of Things Using Piezoelectric Energy Harvesting. *IEEE Access* **2019**, *7*, 94533–94556. [CrossRef]
2. Won, S.S.; Seo, H.; Kawahara, M.; Glinsek, S.; Lee, J.; Kim, Y.; Jeong, C.K.; Kingon, A.I.; Kim, S.H. Flexible vibrational energy harvesting devices using strain-engineered perovskite piezoelectric thin films. *Nano Energy* **2019**, *55*, 182–192. [CrossRef]
3. Sezer, N.; Koç, M. A comprehensive review on the state-of-the-art of piezoelectric energy harvesting. *Nano Energy* **2021**, *80*, 105567. [CrossRef]
4. Brusa, E. Synopsis of the MBSE, Lean and Smart Manufacturing in the Product and Process Design for an Assessment of the Strategy "Industry 4.0". In Proceedings of the INCOSE Italia Conference on Systems Engineering, Rome, Italy, 28–30 November 2018.
5. Zhu, G.; Ren, P.; Hu, J.; Yang, J.; Jia, Y.; Chen, Z.; Ren, F.; Gao, J. Flexible and Anisotropic Strain Sensors with the Asymmetrical Cross-Conducting Network for Versatile Bio-Mechanical Signal Recognition. *ACS Appl. Mater. Interfaces* **2021**, *13*, 44925–44934. [CrossRef] [PubMed]
6. Shabani, E.; Abdekhodaie, S.D.M.J. Laboratory detection methods for the human coronaviruses. *Eur. J. Clin. Microbiol. Infect. Dis.* **2021**, *40*, 225–246. [CrossRef] [PubMed]
7. DeVore, A.D.; Wosik, J.; Hernandez, A.F. The Future of Wearables in Heart Failure Patients. *JACC Heart Fail.* **2019**, *7*, 922–932. [CrossRef]
8. Rao, J.; Chen, Z.; Zhao, D.; Yin, Y.; Wang, X.; Yi, F. Recent Progress in Self-Powered Skin Sensors. *Sensors* **2019**, *19*, 2763. [CrossRef]
9. Promphet, N.; Ummartyotin, S.; Ngeontae, W.; Puthongkham, P.; Rodthongkum, N. Non-invasive wearable chemical sensors in real-life applications. *Anal. Chim. Acta* **2021**, *1179*, 338643. [CrossRef]
10. Kamišalić, A.; Fister, I.; Turkanović, M.; Karakatič, S. Sensors and Functionalities of Non-Invasive Wrist-Wearable Devices: A Review. *Sensors* **2018**, *18*, 1714. [CrossRef]
11. Khan, Y.; Ostfeld, A.E.; Lochner, C.M.; Pierre, A.; Arias, A.C. Monitoring of Vital Signs with Flexible and Wearable Medical Devices. *Adv. Mater.* **2016**, *28*, 4373–4395. [CrossRef]
12. Kim, H.S.; Kim, J.H.; Kim, J. A Review of Piezoelectric Energy Harvesting Based on Vibration. *Int. J. Precis. Eng. Manuf.* **2011**, *12*, 1129–1141. [CrossRef]
13. Pawar, O.Y.; Patil, S.L.; Redekar, R.S.; Patil, S.B.; Lim, S.; Tarwal, N.L. Strategic Development of Piezoelectric Nanogenerator and Biomedical Applications. *Appl. Sci.* **2023**, *13*, 2891. [CrossRef]
14. Zhao, Z.; Dai, Y.; Dou, S.; Liang, J. Flexible nanogenerators for wearable electronic applications based on piezoelectric materials. *Mater. Today Energy* **2021**, *20*, 100690. [CrossRef]
15. Yang, Z.; Zhu, Z.; Chen, Z.; Liu, M.; Zhao, B.; Liu, Y.; Cheng, Z.; Wang, S.; Yang, W.; Yu, T. Recent Advances in Self-Powered Piezoelectric and Triboelectric Sensors: From Material and Structure Design to Frontier Applications of Artificial Intelligence. *Sensors* **2021**, *21*, 8422. [CrossRef]
16. Fan, F.R.; Tian, Z.Q.; Lin Wang, Z. Flexible triboelectric generator. *Nano Energy* **2012**, *1*, 328–334. [CrossRef]
17. Zou, J.; Zhang, M.; Huang, J.; Bian, J.; Jie, Y.; Willander, M.; Cao, X.; Wang, N.; Wang, Z.L. Coupled Supercapacitor and Triboelectric Nanogenerator Boost Biomimetic Pressure Sensor. *Adv. Energy Mater.* **2018**, *8*, 1702671. [CrossRef]

18. Kuang, S.; Suo, X.; Song, P.; Luo, J. Instantaneous Self-Powered Sensing System Based on Planar-Structured Rotary Triboelectric Nanogenerator. *Sensors* **2021**, *21*, 3741. [CrossRef] [PubMed]
19. Toroń, B.; Mistewicz, K.; Jesionek, M.; Kozioł, M.; Zubko, M.; Stróż, D. A new hybrid piezo/triboelectric SbSeI nanogenerator. *Energy* **2022**, *238*, 122048. [CrossRef]
20. Xue, H.; Yang, Q.; Wang, D.; Luo, W.; Wang, W.; Lin, M.; Liang, D.; Luo, Q. A wearable pyroelectric nanogenerator and self-powered breathing sensor. *Nano Energy* **2017**, *38*, 147–154. [CrossRef]
21. Korkmaz, S.; Kariper, I.A. Pyroelectric nanogenerators (PyNGs) in converting thermal energy into electrical energy: Fundamentals and current status. *Nano Energy* **2021**, *84*, 105888. [CrossRef]
22. Yang, Y.; Guo, W.; Pradel, K.C.; Zhu, G.; Zhou, Y.; Zhang, Y.; Hu, Y.; Lin, L.; Wang, Z.L. Pyroelectric Nanogenerators for Harvesting Thermoelectric Energy. *Nano Lett.* **2012**, *12*, 2833–2838. [CrossRef]
23. Lee, M.; Teuscher, J.; Miyasaka, T.; Murakami, T.; Im, J.H. Efficient Hybrid Solar Cells Based on Meso-Superstructured Organometal Halide Perovskites. *Science* **2012**, *338*, 643–647. [CrossRef]
24. Yoon, G.C.; Shin, K.S.; Gupta, M.K.; Lee, K.Y.; Lee, J.H.; Wang, Z.L.; Kim, S.W. High-performance hybrid cell based on an organic photovoltaic device and a direct current piezoelectric nanogenerator. *Nano Energy* **2015**, *12*, 547–555. [CrossRef]
25. Rabaey, J.; Ammer, M.; da Silva, J.; Patel, D.; Roundy, S. PicoRadio supports ad hoc ultra-low power wireless networking. *Computer* **2000**, *33*, 42–48. [CrossRef]
26. Khalid, A.; Redhewal, A.; Kumar, M.; Srivastav, A. Piezoelectric Vibration Harvesters Based on Vibrations of Cantilevered Bimorphs: A Review. *Mater. Sci. Appl.* **2015**, *6*, 818–827. [CrossRef]
27. Holmes, J. Trajectories of spheres in strong winds with application to wind-borne debris. *J. Wind Eng. Ind. Aerodyn.* **2004**, *92*, 9–22. [CrossRef]
28. Raghunathan, V.; Kansal, A.; Hsu, J.; Friedman, J.; Srivastava, M. Design considerations for solar energy harvesting wireless embedded systems. In Proceedings of the IPSN 2005. Fourth International Symposium on Information Processing in Sensor Networks, Boise, ID, USA, 15 April 2005; pp. 457–462. [CrossRef]
29. Paradiso, J.; Starner, T. Energy scavenging for mobile and wireless electronics. *IEEE Pervasive Comput.* **2005**, *4*, 18–27. [CrossRef]
30. Stevens, J.W. Optimized Thermal Design of Small ΔT Thermoelectric Generators. In Proceedings of the 34th Intersociety Energy Conversion Engineering Conference, Vancouver, BC, Canada, 2–5 August 1999; p. 8. [CrossRef]
31. Beeby, S.P.; Tudor, M.J.; White, N.M. Energy harvesting vibration sources for microsystems applications. *Meas. Sci. Technol.* **2006**, *17*, R175. [CrossRef]
32. Beeby, S.; Torah, R.; Tudor, M.; Glynne-Jones, P.; O'Donnell, T.; Saha, C.; Roy, S. Micro electromagnetic generator for vibration energy harvesting. *J. Micromech. Microeng.* **2007**, *17*, 1257. [CrossRef]
33. Delprete, C.; Brusa, E.; Tonoli, A. Modeling for self-sensing electromechanical systems. In Proceedings of the 3rd International Conference on Motion and Vibration Control MOVIC'96, Chiba, Japan, 1–6 September 1996; pp. 117–122.
34. Pasquale, G.D.; Brusa, E.; Soma, A. Capacitive vibration energy harvesting with resonance tuning. In Proceedings of the 2009 Symposium on Design, Test, Integration & Packaging of MEMS/MOEMS, Rome, Italy, 1–3 April 2009; pp. 280–285.
35. Erturk A.; Inman D.J. Introduction to Piezoelectric Energy Harvesting. In *Piezoelectric Energy Harvesting*; John Wiley & Sons, Ltd.: Hoboken, NJ, USA, 2011; Chapter 1, pp. 1–18. [CrossRef]
36. Madinei, H.; Khodaparast, H.H.; Adhikari, S.; Friswell, M. Design of MEMS piezoelectric harvesters with electrostatically adjustable resonance frequency. *Mech. Syst. Signal Process.* **2016**, *81*, 360–374. [CrossRef]
37. Zhou, X.; Parida, K.; Halevi, O.; Liu, Y.; Xiong, J.; Magdassi, S.; Lee, P.S. All 3D-printed stretchable piezoelectric nanogenerator with non-protruding kirigami structure. *Nano Energy* **2020**, *72*, 104676. [CrossRef]
38. Chen, J.; Oh, S.K.; Nabulsi, N.; Johnson, H.; Wang, W.; Ryou, J.H. Biocompatible and sustainable power supply for self-powered wearable and implantable electronics using III-nitride thin-film-based flexible piezoelectric generator. *Nano Energy* **2019**, *57*, 670–679. [CrossRef]
39. Brusa, E.; Carabelli, S.; Carraro, F.; Tonoli, A. Electromechanical Tuning of Self-Sensing Piezoelectric Transducers. *J. Intell. Mater. Syst. Struct.* **1998**, *9*, 198–209. [CrossRef]
40. Wu, N.; Wang, Q.; Xie, X. Ocean wave energy harvesting with a piezoelectric coupled buoy structure. *Appl. Ocean Res.* **2015**, *50*, 110–118. [CrossRef]
41. Sun, Y.; Chen, J.; Li, X.; Lu, Y.; Zhang, S.; Cheng, Z. Flexible piezoelectric energy harvester/sensor with high voltage output over wide temperature range. *Nano Energy* **2019**, *61*, 337–345. [CrossRef]
42. Brusa, E. Design of a kinematic vibration energy harvester for a smart bearing with piezoelectric/magnetic coupling. *Mech. Adv. Mater. Struct.* **2018**, *27*, 1322–1330. [CrossRef]
43. Anton, S.; Sodano, H. A Review of Power Harvesting Using Piezoelectric Materials (2003–2006). *Smart Mater. Struct.* **2007**, *16*, R1. [CrossRef]
44. Covaci, C.; Gontean, A. Piezoelectric energy harvesting solutions: A review. *Sensors* **2020**, *20*, 3512. [CrossRef]
45. Erturk, A.; Inman, D.J. An experimentally validated bimorph cantilever model for piezoelectric energy harvesting from base excitations. *Smart Mater. Struct.* **2009**, *18*, 025009. [CrossRef]
46. Liu, H.; Zhong, J.; Lee, C.; Lee, S.W.; Lin, L. A comprehensive review on piezoelectric energy harvesting technology: Materials, mechanisms, and applications. *Appl. Phys. Rev.* **2018**, *5*, 041306. [CrossRef]

47. Habib, M.; Lantgios, I.; Hornbostel, K. A review of ceramic, polymer and composite piezoelectric materials. *J. Phys. D Appl. Phys.* **2022**, *55*, 423002. [CrossRef]
48. Zhou, Q.; Lam, K.H.; Zheng, H.; Qiu, W.; Shung, K.K. Piezoelectric single crystal ultrasonic transducers for biomedical applications. *Prog. Mater. Sci.* **2014**, *66*, 87–111. [CrossRef] [PubMed]
49. Dawson, L.H. Piezoelectricity of Crystal Quartz. *Phys. Rev.* **1927**, *29*, 532–541. [CrossRef]
50. Haraoubia, B. 3—High-frequency Oscillators. In *Nonlinear Electronics 1*; Haraoubia, B., Ed.; Elsevier: Amsterdam, The Netherlands, 2018; pp. 125–169. [CrossRef]
51. Bunde, R.L.; Jarvi, E.J.; Rosentreter, J.J. Piezoelectric quartz crystal biosensors. *Talanta* **1998**, *46*, 1223–1236. [CrossRef]
52. Dye, D.W. The piezo-electric quartz resonator and its equivalent electrical circuit. *Proc. Phys. Soc. Lond.* **1925**, *38*, 399. [CrossRef]
53. Nicolson, A.M. The Piezo Electric Effect in the Composite Rochelle Salt Crystal. *Trans. Am. Inst. Electr. Eng.* **1919**, *XXXVIII*, 1467–1493. [CrossRef]
54. Andrusyk, A. Piezoelectric Effect in Rochelle Salt. In *Ferroelectrics—Physical Effects*; IntechOpen: London, UK, 2011. [CrossRef]
55. Shur, V. Nano- and Microdomain Engineering of Lithium Niobate and Lithium Tantalate for Piezoelectric Applications. In *Advanced Piezoelectric Materials*, 2nd ed.; Uchino, K., Ed.; Woodhead Publishing: Sawston, UK, 2017; pp. 235–270. [CrossRef]
56. Uchino, K. The Development of Piezoelectric Materials and the New Perspective. In *Advanced Piezoelectric Materials*, 2nd ed.; Uchino, K., Ed.; Woodhead Publishing: Sawston, UK, 2017; pp. 1–92. [CrossRef]
57. Yamada, T.; Niizeki, N.; Toyoda, H. Piezoelectric and Elastic Properties of Lithium Niobate Single Crystals. *Jpn. J. Appl. Phys.* **1967**, *6*, 151. [CrossRef]
58. Safaei, M.; Sodano, H.A.; Anton, S.R. A review of energy harvesting using piezoelectric materials: State-of-the-art a decade later (2008–2018). *Smart Mater. Struct.* **2019**, *28*, 113001. [CrossRef]
59. Wu, W.; Bai, S.; Miaomiao, Y.; Qin, Y.; Wang, Z.; Jing, T. Lead Zirconate Titanate Nanowire Textile Nanogenerator for Wearable Energy-Harvesting and Self-Powered Devices. *ACS Nano* **2012**, *6*, 6231–6235. [CrossRef]
60. Likhon, M.M.; Shawan, S.I.; Alam, M.N.S.B.; Siddique, S. Characterizing Piezoelectric Properties of PZT-4, PZT-5A, PZT-5J, PZT-7A and Lithium Tantalate Material-based Transducers. In Proceedings of the International Conference on Green Energy, Computing and Sustainable Technology, GECOST 2021, Miri, Malaysia, 7–9 July 2021.
61. Sunithamani, S.; Lakshmi, P.; Flora, E.E. PZT length optimization of MEMS piezoelectric energy harvester with a non-traditional cross section: Simulation study. *Microsyst. Technol.* **2013**, *20*, 2165–2171. [CrossRef]
62. Naduvinamani, S.; Iyer, N.C. Design and simulation of PZT based MEMS piezoelectric accelerometer. In Proceedings of the International Conference on Electrical, Electronics, and Optimization Techniques, ICEEOT 2016, Chennai, India, 3–5 March 2016; pp. 3715–3721.
63. Huang, J.; Yao, M.; Yao, X. A novel approach to improving the electromechanical properties of PZT-based piezoelectric ceramics via a grain coating modification strategy. *Ceram. Int.* **2021**, *47*, 16294–16302. [CrossRef]
64. Mengwei, L.; Tianhong, C.; Weijie, D.; Yan, C.; Jing, W.; Liqun, D.; Liding, W. Piezoelectric microcantilevers with Two PZT thin-film elements for microsensors and microactuators. In Proceedings of the 1st IEEE International Conference on Nano Micro Engineered and Molecular Systems, Zhuhai, China, 18–21 January 2006; pp. 775–778.
65. Kanno, I. Piezoelectric Pzt Thin Films: Deposition, Evaluation and Their Applications. In Proceedings of the 2019 20th International Conference on Solid-State Sensors, Actuators and Microsystems & Eurosensors XXXIII (TRANSDUCERS & EUROSENSORS XXXIII), Berlin, Germany, 23–27 June 2019; pp. 785–788. [CrossRef]
66. Low, T.; Guo, W. Modeling of a three-layer piezoelectric bimorph beam with hysteresis. *J. Microelectromech. Syst.* **1995**, *4*, 230–237. [CrossRef]
67. Butt, Z.; Pasha, A.; Qayyum, F.; Anjum, Z.; Ahmad, N.; Elahi, H. Generation of electrical energy using lead zirconate titanate (PZT-5A) piezoelectric material: Analytical, numerical and experimental verifications. *J. Mech. Sci. Technol.* **2016**, *30*, 3553–3558. [CrossRef]
68. Zhu, X. Piezoelectric ceramic materials: Processing, properties, characterization, and applications. In *Piezoelectric Materials: Structure, Properties and Applications*; Nova Science Publishers: Hauppauge, NY, USA, 2010; pp. 1–36.
69. Huisman, J.; Magalini, F.; Kuehr, R.; Maurer, C.; Ogilvie, S.; Poll, J.; Delgado, C.; Artim, E.; Szlezak, J.; Stevels, A. *Review of Directive 2002/96 on Waste Electrical and Electronic Equipment (WEEE)*; United Nations University: Tokyo, Japan, 2008; Volume 37.
70. Shrout, T.; Zhang, S. Lead-Free Piezoelectric Ceramics: Alternatives for PZT? *J. Electroceram.* **2007**, *19*, 113–126. [CrossRef]
71. Akdogan, E.; Kerman, K.; Abazari, M.; Safari, A. Origin of High Piezoelectric Activity in Ferroelectric $(K_{0.44}Na_{0.52}Li_{0.04})$-$(Nb_{0.84}Ta_{0.1}Sb_{0.06})O_3$ Ceramics. *Appl. Phys. Lett.* **2008**, *92*, 112908. [CrossRef]
72. Carreño-Jiménez, B.; Benítez-Benítez, J.L.; Castañeda-Guzmán, R.; Acuautla, M.; López-Juárez, R. Lead-free KNN-based thin films obtained by pulsed laser deposition. In Proceedings of the 2022 IEEE International Symposium on Applications of Ferroelectrics (ISAF), Tours, France, 27 June–1 July 2022; pp. 1–4. [CrossRef]
73. Saito, Y.; Takao, H.; Tani, T.; Nonoyama, T.; Takatori, K.; Homma, T.; Nagaya, T.; Nakamura, M. Lead-free piezoceramics. *Nature* **2004**, *432*, 84–87. [CrossRef] [PubMed]
74. Smeltere, I.; Antonova, M.; Dunce, M.; Livinsh, M.; Garbarz-Glos, B. Electrical and mechanical properties of KNN based lead-free ceramics. In Proceedings of the 12th Conference of the European Ceramic Society—ECerS XII, Stockholm, Sweden, 19–23 June 2011.

75. Rodel, J.; Jo, W.; Seifert, K.; Anton, E.M.; Granzow, T.; Damjanovic, D. Perspective on the Development of Lead-Free Piezoceramics. *J. Am. Ceram. Soc.* **2009**, *92*, 1153–1177. [CrossRef]
76. Li, P.; Huan, Y.; Yang, W.; Zhu, F.; Li, X.; Zhang, X.; Shen, B.; Zhai, J. High-performance potassium-sodium niobate lead-free piezoelectric ceramics based on polymorphic phase boundary and crystallographic texture. *Acta Mater.* **2018**, *165*, 486–495. [CrossRef]
77. Acosta, M.; Novak, N.; Rojas, V.; Patel, S.; Vaish, R.; Koruza, J.; Rossetti, G.A., Jr.; Rödel, J. $BaTiO_3$-based piezoelectrics: Fundamentals, current status, and perspectives. *Appl. Phys. Rev.* **2017**, *4*, 041305. [CrossRef]
78. Baek, C.; Park, H.; Yun, J.H.; Kim, D.K.; Park, K.I. Lead-free $BaTiO_3$ Nanowire Arrays-based Piezoelectric Energy Harvester. *MRS Adv.* **2017**, *2*, 1–6. [CrossRef]
79. Hiruma, Y.; Nagata, H.; Takenaka, T. Thermal Depoling Process and Piezoelectric Properties of Bismuth Sodium Titanate Ceramics. *J. Appl. Phys.* **2009**, *105*, 084112–084112. [CrossRef]
80. Safari, A.; Abazari, M. Lead-Free Piezoceramic Ceramics and Thin Films. *Ultrason. Ferroelectr. Freq. Control IEEE Trans.* **2010**, *57*, 2165–2176. [CrossRef] [PubMed]
81. Reichmann, K.; Feteira, A.; Li, M. Bismuth Sodium Titanate Based Materials for Piezoelectric Actuators. *Materials* **2015**, *8*, 8467–8495. [CrossRef] [PubMed]
82. Gao, J.; Xue, D.; Liu, W.; Zhou, C.; Ren, X. Recent Progress on $BaTiO_3$-Based Piezoelectric Ceramics for Actuator Applications. *Actuators* **2017**, *6*, 24. [CrossRef]
83. Karaki, T.; Yan, K.; Miyamoto, T.; Adachi, M. Lead-Free Piezoelectric Ceramics with Large Dielectric and Piezoelectric Constants Manufactured from $BaTiO_3$ Nano-Powder. *Jpn. J. Appl. Phys.* **2007**, *46*, L97–L98. [CrossRef]
84. Liu, W.; Ren, X. Large Piezoelectric Effect in Pb-Free Ceramics. *Phys. Rev. Lett.* **2009**, *103*, 257602. [CrossRef] [PubMed]
85. He, H.; Lu, W.; Oh, J.A.S.; Li, Z.; Lu, X.; Zeng, K.; Lu, L. Probing the Coexistence of Ferroelectric and Relaxor State in $Bi_{0.5}Na_{0.5}TiO_3$-Based Ceramics for Enhanced Piezoelectric Performance. *Acs Appl. Mater. Interfaces* **2020**, *12*, 30548–30556. [CrossRef]
86. Matsumoto, K.; Hiruma, Y.; Nagata, H.; Takenaka, T. Piezoelectric Properties of $KNbO_3$ Ceramics Prepared by Ordinary Sintering. *Ferroelectrics* **2007**, *358*, 169–174. [CrossRef]
87. Nakamura, K.; Tokiwa, T.; Kawamura, Y. Domain structures in $KNbO_3$ crystals and their piezoelectric properties. *J. Appl. Phys.* **2002**, *91*, 9272–9276. [CrossRef]
88. Wada, S.; Seike, A.; Tsurumi, T. Poling Treatment and Piezoelectric Properties of Potassium Niobate Ferroelectric Single Crystals. *Jpn. J. Appl. Phys.* **2001**, *40*, 5690–5697. [CrossRef]
89. Guan, S.; Yang, H.; Cheng, S.; Wang, X.; Sun, Y.; Yang, X.; Tan, H.; Zhang, H. Phase structure, domain structure, thermal stability, and high-temperature piezoelectric response of $BiFeO_3$–$BaTiO_3$ lead-free piezoelectric ceramics. *Ceram. Int.* **2023**, *50*, 384–393. [CrossRef]
90. Neaton, J.; Ederer, C.; Waghmare, U.; Spaldin, N.; Rabe, K. First-Principles Study of Spontaneous Polarization in Multiferroic $BiFeO_3$. *Phys. Rev. B* **2004**, *71*, 014113. [CrossRef]
91. Wu, J.; Fan, Z.; Xiao, D.; Zhu, J.; Wang, J. Multiferroic bismuth ferrite-based materials for multifunctional applications: Ceramic bulks, thin films and nanostructures. *Prog. Mater. Sci.* **2016**, *84*, 335–402. [CrossRef]
92. Gerfers, F.; Kohlstadt, P.; Ginsburg, E.; He, M.; Samara-Rubio, D.; Manoli, Y.; Wang, L. *Sputtered AlN Thin Films for Piezoelectric MEMS Devices—FBAR Resonators and Accelerometers*; IntechOpen: London, UK, 2010. [CrossRef]
93. Guy, I.; Muensit, N.; Goldys, E. Extensional Piezoelectric Coefficients of Gallium Nitride and Aluminum Nitride. *Appl. Phys. Lett.* **2000**, *75*, 4133–4135. [CrossRef]
94. Tittmann, B.R.; Parks, D.A.; Zhang, S. High Temperature Piezoelectrics—A Comparison. In Proceedings of the 13th International Symposium on Nondestructive Characterization of Materials (NDCM-XIII), Le Mans, France, 20–24 May 2013.
95. Yarar, E.; Hrkac, V.; Zamponi, C.; Piorra, A.; Kienle, L.; Quandt, E. Low temperature aluminum nitride thin films for sensory applications. *AIP Adv.* **2016**, *6*, 075115. [CrossRef]
96. Ahmad, M.A.; Plana, R. Vertical displacement detection of an aluminum nitride piezoelectric thin film using capacitance measurements. *Int. J. Microw. Wirel. Technol.* **2009**, *1*, 5–9. [CrossRef]
97. Wang, R.; Bhave, S.A.; Bhattacharjee, K. Design and Fabrication of S0 Lamb-Wave Thin-Film Lithium Niobate Micromechanical Resonators. *J. Microelectromech. Syst.* **2015**, *24*, 300–308. [CrossRef]
98. Plessky, V.; Yandrapalli, S.; Turner, P.; Villanueva, L.G.; Koskela, J.; Hammond, R. 5 GHz laterally-excited bulk-wave resonators (XBARs) based on thin platelets of Lithium Niobate. *Electron. Lett.* **2019**, *55*, 98–100. [CrossRef]
99. Yang, Y.; Lu, R.; Manzaneque, T.; Gong, S. Toward Ka Band Acoustics: Lithium Niobate Asymmetrical Mode Piezoelectric MEMS Resonators. In Proceedings of the 2018 IEEE International Frequency Control Symposium (IFCS), Olympic Valley, CA, USA, 21–24 May 2018; pp. 1–5. [CrossRef]
100. Yamada, T.; Iwasaki, H.; Niizeki, N. Piezoelectric and Elastic Properties of $LiTaO_3$: Temperature Characteristics. *Jpn. J. Appl. Phys.* **1969**, *8*, 1127. [CrossRef]
101. Bartasyte, A.; Margueron, S.; Baron, T.; Oliveri, S.; Boulet, P. Toward High-Quality Epitaxial $LiNbO_3$ and $LiTaO_3$ Thin Films for Acoustic and Optical Applications. *Adv. Mater. Interfaces* **2017**, *4*, 1600998. [CrossRef]
102. Yamashita, Y.Y.Y. Large Electromechanical Coupling Factors in Perovskite Binary Material System. *Jpn. J. Appl. Phys.* **1994**, *33*, 5328. [CrossRef]

103. Agrawal, R.; Horacio, D. Giant Piezoelectric Size Effects in Zinc Oxide and Gallium Nitride Nanowires. A First Principles Investigation. *Nano Lett.* **2011**, *11*, 786–790. [CrossRef] [PubMed]
104. Zhou, J.; Fei, P.; Gao, Y.; Gu, Y.; Liu, J.; Bao, G.; Wang, Z. Mechanical–Electrical Triggers and Sensors Using Piezoelectric Micowires/Nanowires. *Nano Lett.* **2008**, *8*, 2725–2730. [CrossRef] [PubMed]
105. Kou, L.z.; Guo, W.l.; Li, C. Piezoelectricity of ZnO and its nanostructures. In Proceedings of the 2008 Symposium on Piezoelectricity, Acoustic Waves, and Device Applications, Nanjing, China, 5–8 December 2008; pp. 354–359. [CrossRef]
106. Wang, Z.L.; Song, J. Piezoelectric Nanogenerators Based on Zinc Oxide Nanowire Arrays. *Science* **2006**, *312*, 242–246. [CrossRef] [PubMed]
107. Khudiar, A.; Khalaf, M.; Ofui, A. Improvement of the sensing characterizations of ZnO nanostructure by using thermal annealing prepared through R. F. magnetron sputtering technique. *Opt. Mater.* **2021**, *114*, 110885. [CrossRef]
108. Ayman, M. The enhancement of nonlinear absorption of Zn/ZnO thin film by creation oxygen vacancies via infrared laser irradiation and coating with Ag thin film via pulsed laser deposition. *J. Mol. Struct.* **2021**, *1226*, 129407. [CrossRef]
109. Alanthattil, A.; Patil, P.; Gummagol, N.; Goutam, U.; Sharma, P.; B V, R. Microstructural, linear and nonlinear optical study of spray pyrolysed nanostructured La–ZnO thin film: An effect of deposition temperature. *Opt. Mater.* **2021**, *122*, 111742. [CrossRef]
110. Wang, J.; He, Y.c.; Luo, T.C.; Li, Y.; Zhou, Z.; Fan, B.f.; Li, J.; Wang, G. Simulation and experimental verification study on the process parameters of ZnO-MOCVD. *Ceram. Int.* **2021**, *47*, 15471–15482. [CrossRef]
111. Li, Q.; Ying, M.; Zhang, M.; Cheng, W.; Li, W.; Liao, B.; Zhang, x. Structural characterization and surface polarity determination of polar ZnO films prepared by MBE. *Appl. Nanosci.* **2021**, *13*, 3197–3204. [CrossRef]
112. Cholleti, E. A Review on 3D printing of piezoelectric materials. *IOP Conf. Ser. Mater. Sci. Eng.* **2018**, *455*, 012046. [CrossRef]
113. Sappati, K.K.; Bhadra, S. Piezoelectric Polymer and Paper Substrates: A Review. *Sensors* **2018**, *18*, 3605. [CrossRef] [PubMed]
114. Fotouhi, S.; Akrami, R.; Ferreira-Green, K.; Naser, G.A.M.; Fotouhi, M.; Fragassa, C. Piezoelectric PVDF sensor as a reliable device for strain/load monitoring of engineering structures. *IOP Conf. Ser. Mater. Sci. Eng.* **2019**, *659*, 012085. [CrossRef]
115. Koga, K.; Ohigashi, H. Piezoelectricity and related properties of vinylidene fluoride and trifluoroethylene copolymers. *J. Appl. Phys.* **1986**, *59*, 2142–2150. [CrossRef]
116. Elahi, H.; Eugeni, M.; Gaudenzi, P. A Review on Mechanisms for Piezoelectric-Based Energy Harvesters. *Energies* **2018**, *11*, 1850. [CrossRef]
117. Ruan, L.; Yao, X.; Chang, Y.; Zhou, L.; Qin, G.; Zhang, X. Properties and Applications of the β Phase Poly(vinylidene fluoride). *Polymers* **2018**, *10*, 228. [CrossRef]
118. Sajkiewicz, P. Crystallization behaviour of poly(vinylidene fluoride). *Eur. Polym. J.* **1999**, *35*, 1581–1590. [CrossRef]
119. Gradys, A.; Sajkiewicz, P.; Adamovsky, S.; Minakov, A.; Schick, C. Crystallization of poly(vinylidene fluoride) during ultra-fast cooling. *Thermochim. Acta* **2007**, *461*, 153–157. [CrossRef]
120. Siddiqui, S.; Kim, D.I.; Roh, E.; Duy, L.T.; Trung, T.Q.; Nguyen, M.T.; Lee, N.E. A Durable and Stable Piezoelectric Nanogenerator with Nanocomposite Nanofibers Embedded in an Elastomer under High Loading for a Self-Powered Sensor System. *Nano Energy* **2016**, *30*, 434–442. [CrossRef]
121. Jain, A.; Kumar, J.; Mahapatra, D.; Rathod, V. *Development of P(VDF-Trfe) Films and Its Quasi-Static and Dynamic Strain Response*; IJERT: Gandhinagar, India, 2013.
122. Dahiya, R.; Valle, M.; Metta, G.; Lorenzelli, L.; Pedrotti, S. Deposition, processing and characterization of P(VDF-TrFE) thin films for sensing applications. In Proceedings of the SENSORS, 2008 IEEE, Lecce, Italy, 26–29 October 2008; pp. 490–493. [CrossRef]
123. Fang, F.; Shan, S.C.; Yang, W. A multipeak phenomenon of magnetoelectric coupling in Terfenol-D/P(VDF-TrFE)/Terfenol-D laminates. *J. Appl. Phys.* **2010**, *108*, 104505. [CrossRef]
124. Lovinger, A.J. Ferroelectric transition in a copolymer of vinylidene fluoride and tetrafluoroethylene. *Macromolecules* **1983**, *16*, 1529–1534. [CrossRef]
125. Lovinger, A.J.; Davis, D.D.; Cais, R.E.; Kometani, J.M. Compositional variation of the structure and solid-state transformations of vinylidene fluoride/tetrafluoroethylene copolymers. *Macromolecules* **1988**, *21*, 78–83. [CrossRef]
126. Lovinger, A.J.; Johnson, G.E.; Bair, H.E.; Anderson, E.W. Structural, dielectric, and thermal investigation of the Curie transition in a tetrafluoroethylene copolymer of vinylidene fluoride. *J. Appl. Phys.* **1984**, *56*, 2412–2418. [CrossRef]
127. Green, J.; Rabolt, J.F. Identification of a Curie transition in vinylidene fluoride/tetrafluoroethylene random copolymers by spectroscopic methods. *Macromolecules* **1987**, *20*, 456–457. [CrossRef]
128. Lando, J.B.; Doll, W.W. The polymorphism of poly(vinylidene fluoride). I. The effect of head-to-head structure. *J. Macromol. Sci. Part B* **1968**, *2*, 205–218. [CrossRef]
129. Nalwa, H.S. *Crystal Structure and Phase Transition of PVDF and Related Copolymers*; CRC Press: Boca Raton, FL, USA, 1995.
130. Lovinger, A.J. Ferroelectric Polymers. *Science* **1983**, *220*, 1115–1121. [CrossRef]
131. Tai, Y.; Yang, S.; Yu, S.; Banerjee, A.; Myung, N.; Nam, J. Modulation of piezoelectric properties in electrospun PLLA nanofibers for application-specific self-powered stem cell culture platforms. *Nano Energy* **2021**, *89*, 106444. [CrossRef]
132. Li, J.; Long, Y.; Yang, F.; Wang, X. Degradable Piezoelectric Biomaterials for Wearable and Implantable Bioelectronics. *Curr. Opin. Solid State Mater. Sci.* **2020**, *24*, 100806. [CrossRef]
133. Bajpai, A.K.; Bajpai, J.; Saini, R.; Gupta, R. Responsive Polymers in Biology and Technology. *Polym. Rev.* **2011**, *51*, 53–97. [CrossRef]

134. Yoshida, T.; Imoto, K.; Tahara, K.; Naka, K.; Uehara, Y.; Kataoka, S.; Date, M.; Fukada, E.; Tajitsu, Y. Piezoelectricity of Poly(L-lactic Acid) Composite Film with Stereocomplex of Poly(L-lactide) and Poly(D-lactide). *Jpn. J. Appl. Phys.* **2010**, *49*, 09MC11. [CrossRef]
135. Zhao, L.J.; Tang, C.P.; Gong, P. Correlation of Direct Piezoelectric Effect on EAPap under Ambient Factors. *Int. J. Autom. Comput.* **2010**, *7*, 324–329. [CrossRef]
136. Hassan, S.; Voon, L.; Velayutham, T.S.; Zhai, L.; Kim, H.C.; Kim, J. Review of Cellulose Smart Material: Biomass Conversion Process and Progress on Cellulose-Based Electroactive Paper. *J. Renew. Mater.* **2017**, *6*, 1–25. [CrossRef]
137. Csoka, L.; Hoeger, I.C.; Rojas, O.J.; Peszlen, I.; Pawlak, J.J.; Peralta, P.N. Piezoelectric Effect of Cellulose Nanocrystals Thin Films. *ACS Macro Lett.* **2012**, *1*, 867–870. [CrossRef]
138. Mahadeva, S.K.; Walus, K.; Stoeber, B. Piezoelectric Paper Fabricated via Nanostructured Barium Titanate Functionalization of Wood Cellulose Fibers. *ACS Appl. Mater. Interfaces* **2014**, *6*, 7547–7553. [CrossRef]
139. Kapat, K.; Shubhra, Q.T.H.; Zhou, M.; Leeuwenburgh, S. Piezoelectric Nano-Biomaterials for Biomedicine and Tissue Regeneration. *Adv. Funct. Mater.* **2020**, *30*, 1909045. [CrossRef]
140. Jain, A.; Prashanth, K.J.; Sharma, A.K.; Jain, A.; Rashmi, P.N. Dielectric and piezoelectric properties of PVDF/PZT composites: A review. *Polym. Eng. Sci.* **2015**, *55*, 1589–1616. [CrossRef]
141. Yoon, S.; Shin, D.J.; Ko, Y.H.; Cho, K.H.; Koh, J.H. Flexible Energy Harvester Based on Poly(vinylidene fluoride) Composite Films. *J. Nanosci. Nanotechnol.* **2019**, *19*, 1289–1294. [CrossRef] [PubMed]
142. Smith, W. The role of piezocomposites in ultrasonic transducers. In Proceedings of the Proceedings, IEEE Ultrasonics Symposium, Montreal, QC, Canada, 3–6 October 1989; Volume 2, pp. 755–766. [CrossRef]
143. Tian, G.; Deng, W.; Gao, Y.; Xiong, D.; Yan, C.; He, X.; Yang, T.; Jin, L.; Chu, X.; Zhang, H.; et al. Rich lamellar crystal baklava-structured PZT/PVDF piezoelectric sensor toward individual table tennis training. *Nano Energy* **2019**, *59*, 574–581. [CrossRef]
144. Wankhade, S.H.; Tiwari, S.; Gaur, A.; Maiti, P. PVDF–PZT nanohybrid based nanogenerator for energy harvesting applications. *Energy Rep.* **2020**, *6*, 358–364. [CrossRef]
145. Li, J.; Chen, S.; Liu, W.; Fu, R.; Tu, S.; Zhao, Y.; Dong, L.; Yan, B.; Gu, Y. High Performance Piezoelectric Nanogenerators Based on Electrospun ZnO Nanorods/PVDF Composite Membranes. *J. Phys. Chem. C* **2019**, *123*, 11378–11387. [CrossRef]
146. Fu, Y.; Cheng, Y.; Chen, C.; Li, D.; Zhang, W. Study on preparation process and enhanced piezoelectric performance of pine-needle-like ZnO@PVDF composite nanofibers. *Polym. Test.* **2022**, *108*, 107513. [CrossRef]
147. Chelu, M.; Stroescu, H.; Anastasescu, M.; Calderon-Moreno, J.; Preda, S.; Stoica, M.; Fogarassy, Z.; Petrik, P.; Gheorghe, M.; Parvulescu, C.; et al. High-quality PMMA/ZnO NWs piezoelectric coating on rigid and flexible metallic substrates. *Appl. Surf. Sci.* **2020**, *529*, 147135. [CrossRef]
148. Zhang, S.; Shen, Y.; Fang, H.; Xu, S.; Song, J.; Wang, Z.L. Growth and replication of ordered ZnO nanowire arrays on general flexible substrates. *J. Mater. Chem.* **2010**, *20*, 10606–10610. [CrossRef]
149. Ou, C.; Sánchez-Jiménez, P.; Datta, A.; Boughey, C.; Whiter, R.; Sahonta, S.; Kar-Narayan, S. Template-Assisted Hydrothermal Growth of Aligned Zinc Oxide Nanowires for Piezoelectric Energy Harvesting Applications. *ACS Appl. Mater. Interfaces* **2016**, *8*, 13678–13683. [CrossRef]
150. Chorsi, M.T.; Curry, E.J.; Chorsi, H.T.; Das, R.; Baroody, J.; Purohit, P.K.; Ilies, H.; Nguyen, T.D. Piezoelectric Biomaterials for Sensors and Actuators. *Adv. Mater.* **2019**, *31*, 1802084. [CrossRef]
151. Perez-Lopez, C.A.; Perez-Taborda, J.A.; Labre, C.; Marmolejo-Tejada, J.M.; Jaramillo-Botero, A.; Avila, A. ZnO/PDMS nanocomposite generator: Interphase influence in the nanocomposite electro-mechanical properties and output voltage. *Energy Rep.* **2021**, *7*, 896–903. [CrossRef]
152. Miranda, I.; Souza, A.; Sousa, P.J.; Ribeiro, J.; Castanheira, E.M.S.; Lima, R.A.; Minas, G.M.H. Properties and Applications of PDMS for Biomedical Engineering: A Review. *J. Funct. Biomater.* **2021**, *13*, 2. [CrossRef] [PubMed]
153. Kuddannaya, S.; Bao, J.; Zhang, Y. Enhanced In Vitro Biocompatibility of Chemically Modified Poly(dimethylsiloxane) Surfaces for Stable Adhesion and Long-term Investigation of Brain Cerebral Cortex Cells. *ACS Appl. Mater. Interfaces* **2015**, *7*, 25529–25538. [CrossRef]
154. Shaukat, H.; Ali, A.; Bibi, S.; Altabey, W.A.; Noori, M.; Kouritem, S.A. A Review of the Recent Advances in Piezoelectric Materials, Energy Harvester Structures, and Their Applications in Analytical Chemistry. *Appl. Sci.* **2023**, *13*, 1300. [CrossRef]
155. Aabid, A.; Raheman, M.A.; Ibrahim, Y.E.; Anjum, A.; Hrairi, M.; Parveez, B.; Parveen, N.; Mohammed Zayan, J. A Systematic Review of Piezoelectric Materials and Energy Harvesters for Industrial Applications. *Sensors* **2021**, *21*, 4145. [CrossRef] [PubMed]
156. Kabakov, P.; Kim, T.; Cheng, Z.; Jiang, X.; Zhang, S. The Versatility of Piezoelectric Composites. *Annu. Rev. Mater. Res.* **2023**, *53*, 165–194. [CrossRef]
157. Mishra, S.; Unnikrishnan, L.; Nayak, S.K.; Mohanty, S. Advances in Piezoelectric Polymer Composites for Energy Harvesting Applications: A Systematic Review. *Macromol. Mater. Eng.* **2019**, *304*, 1800463. [CrossRef]
158. Shashank, P.; Inman, D.J. *Energy Harvesting Technologies*; Springer US: Boston, MA, USA, 2009.
159. Roundy, S.; Wright, P.K. A piezoelectric vibration based generator for wireless electronics. *Smart Mater. Struct.* **2004**, *13*, 1131–1142. [CrossRef]
160. Brusa, E.; Zelenika, S.; Moro, L.; Benasciutti, D. Analytical characterization and experimental validation of performances of piezoelectric vibration energy scavengers. In Proceedings of the Smart Sensors, Actuators, and MEMS IV. International Society for Optics and Photonics, Dresden, Germany, 4–6 May 2009; 2009; Volume 7362, p. 736204. [CrossRef]

161. Uddin, M.N.; Islam, M.; Sampe, J.; Wahab, S.; Ali, S. Proof mass effect on piezoelectric cantilever beam for vibrational energy harvesting using Finite Element Method. In Proceedings of the 2016 International Conference on Radar, Antenna, Microwave, Electronics, and Telecommunications (ICRAMET), Jakarta, Indonesia, 3–5 October 2016; pp. 17–21. [CrossRef]
162. Brusa, E.; Carrera, A.; Delprete, C. Integrated mechatronic design of an industrial piezoelectric vibration energy harvester. *Mech. Adv. Mater. Struct.* **2023** , 1–15. [CrossRef]
163. Erturk, A.; Inman, D.J. A Distributed Parameter Electromechanical Model for Cantilevered Piezoelectric Energy Harvesters. *J. Vib. Acoust.* **2008**, *130*, 041002. [CrossRef]
164. Goldschmidtboeing, F.; Woias, P. Characterization of different beam shapes for piezoelectric energy harvesting. *J. Micromech. Microeng.* **2008**, *18*, 104013. [CrossRef]
165. Mateu, L.; Moll, F. Review of energy harvesting techniques and applications for microelectronics. In Proceedings of the VLSI Circuits and Systems II, International Society for Optics and Photonics, Sevilla, Spain, 9–11 May 2005; Volume 5837, pp. 359–373. [CrossRef]
166. Shahruz, S. Design of mechanical band-pass filters for energy scavenging. *J. Sound Vib.* **2006**, *292*, 987–998. [CrossRef]
167. Askari, M.; Brusa, E.; Delprete, C. Design and modeling of a novel multi-beam piezoelectric smart structure for vibration energy harvesting. *Mech. Adv. Mater. Struct.* **2022**, *29*, 7519–7541. [CrossRef]
168. Askari, M.; Brusa, E.; Delprete, C. Vibration energy harvesting via piezoelectric bimorph plates: An analytical model. *Mech. Adv. Mater. Struct.* **2022**, *30*, 4764–4785. [CrossRef]
169. Askari, M.; Brusa, E.; Delprete, C. On wave propagation and free vibration of piezoelectric sandwich plates with perfect and porous functionally graded substrates. *J. Intell. Mater. Syst. Struct.* **2022**, *33*, 2049–2073. [CrossRef]
170. Askari, M.; Brusa, E.; Delprete, C. On the vibration analysis of coupled transverse and shear piezoelectric functionally graded porous beams with higher-order theories. *J. Strain Anal. Eng. Des.* **2021**, *56*, 29–49. [CrossRef]
171. Askari, M.; Brusa, E.; Delprete, C. Electromechanical Vibration Characteristics of Porous Bimorph and Unimorph Doubly Curved Panels. *Actuators* **2020**, *9*, 7. [CrossRef]
172. Marco, G. Caratterizzazione Elettromeccanica Numerico—Sperimentale di Travi Piezoelettriche Ottimizzate per il Recupero di Energia da Vibrazioni. Ph.D. Thesis, UniversitÀ degli Studi di Udine, Udine, Italy, 2014.
173. Roundy, S.; Leland, E.; Baker, J.; Carleton, E.; Reilly, E.; Lai, E.; Otis, B.; Rabaey, J.; Wright, P.; Sundararajan, V. Improving power output for vibration-based energy scavengers. *IEEE Pervasive Comput.* **2005**, *4*, 28–36. [CrossRef]
174. Benasciutti, D.; Moro, L.; Zelenika, S.; Brusa, E. Vibration energy scavenging via piezoelectric bimorphs of optimized shapes. *Microsyst. Technol.* **2010**, *16*, 657–668. [CrossRef]
175. Matova, S.; Renaud, M.; Jambunathan, M.; Goedbloed, M.; Schaijk, R. Effect of length/width ratio of tapered beams on the performance of piezoelectric energy harvesters. *Smart Mater. Struct.* **2013**, *22*, 075015. [CrossRef]
176. Gogoi, U.J.; Shanmuganantham, T. Energy harvesting of cantilever with silicon tip mass based MEMS energy scavengers. In Proceedings of the 2015 2nd International Conference on Electronics and Communication Systems (ICECS), Coimbatore, India, 26–27 February 2015; pp. 185–188. [CrossRef]
177. Xu, C.; Li, Y.; Yang, T. Optimization of Non-Uniform Deformation on Piezoelectric Circular Diaphragm Energy Harvester with a Ring-Shaped Ceramic Disk. *Micromachines* **2020**, *11*, 963. [CrossRef]
178. Kamal, P.N.M.; Buniyamin, N. Using Piezoelectric Elements as Footsteps Energy Harvester: An Investigation. In Proceedings of the 2018 IEEE 8th International Conference on System Engineering and Technology (ICSET), Bandung, Indonesia, 15–16 October 2018, pp. 1–6. [CrossRef]
179. Li, H.; Tian, C.; Deng, Z.D. Energy harvesting from low frequency applications using piezoelectric materials. *Appl. Phys. Rev.* **2014**, *1*, 041301. [CrossRef]
180. Sugawara, Y.; Onitsuka, K.; Yoshikawa, S.; Xu, Q.; Newnham, R.; Uchino, K. Metal–Ceramic Composite Actuators. *J. Am. Ceram. Soc.* **2005**, *75*, 996–998. [CrossRef]
181. Arnold, D.; Kinsel, W.; Clark, W.; Mo, C. Exploration of New Cymbal Design in Energy Harvesting. *Proc. SPIE Int. Soc. Opt. Eng.* **2011**, *79770T* . [CrossRef]
182. Shim, H.; Kim, K.; Seo, H.; Roh, Y. Equivalent Circuit to Analyze the Transmitting Characteristics of a Cymbal Array. *Sensors* **2022**, *22*, 8743. [CrossRef] [PubMed]
183. Puscasu, O.; Counsell, N.; Herfatmanesh, M.R.; Peace, R.; Patsavellas, J.; Day, R. Powering Lights with Piezoelectric Energy-Harvesting Floors. *Energy Technol.* **2018**, *6*, 906–916. [CrossRef]
184. Sharpes, N.; Vučković, D.; Priya, S. Floor Tile Energy Harvester for Self-Powered Wireless Occupancy Sensing. *Energy Harvest. Syst.* **2016**, *3*, 43–60. [CrossRef]
185. Selim, K.K.; Yehia, H.M.; Abdalfatah, S. Human Footsteps-based Energy Harvesting Using Piezoelectric Elements. In Proceedings of the 2023 International Telecommunications Conference (ITC-Egypt), Alexandria, Egypt, 18–20 July 2023; pp. 140–144. [CrossRef]
186. Chen, Z.; Qian, X.; Song, X.; Jiang, Q.; Huang, R.; Yang, Y.; Li, R.; Shung, K.K.; Chen, Y.; Zhou, Q. Three-Dimensional Printed Piezoelectric Array for Improving Acoustic Field and Spatial Resolution in Medical Ultrasonic Imaging. *Micromachines* **2019**, *10*, 170. [CrossRef]
187. Keshmiri, A.; Deng, X.; Wu, N. New energy harvester with embedded piezoelectric stacks. *Compos. Part B Eng.* **2019**, *163*, 303–313. [CrossRef]

188. Wang, C.; Song, Z.; Gao, Z.; Yu, G.; Wang, S. Preparation and performance research of stacked piezoelectric energy-harvesting units for pavements. *Energy Build.* **2019**, *183*, 581–591. [CrossRef]
189. Xu, T.B.; Siochi, E.J.; Kang, J.H.; Zuo, L.; Zhou, W.; Tang, X.; Jiang, X. Energy harvesting using a PZT ceramic multilayer stack. *Smart Mater. Struct.* **2013**, *22*, 065015. [CrossRef]
190. Yang, H.; Wang, L.; Hou, Y.; Guo, M.; Ye, Z.; Tong, X.; Wang, D. Development in Stacked-Array-Type Piezoelectric Energy Harvester in Asphalt Pavement. *J. Mater. Civ. Eng.* **2017**, *29*, 04017224. [CrossRef]
191. Cascetta, F.; Lo Schiavo, A.; Minardo, A.; Musto, M.; Rotondo, G.; Calcagni, A. Analysis of the energy extracted by a harvester based on a piezoelectric tile. *Curr. Appl. Phys.* **2018**, *18*, 905–911. [CrossRef]
192. Ansari, M.H.; Karami, M.A. Experimental investigation of fan-folded piezoelectric energy harvesters for powering pacemakers. *Smart Mater. Struct.* **2017**, *26*, 065001. [CrossRef]
193. Dong, T.; Halvorsen, E.; Yang, Z. A MEMS-based spiral piezoelectric energy harvester. In Proceedings of the PowerMEMS 2008 + microEMS2008, Sendai, Japan, 9–12 November 2008; pp. 77–80.
194. Udvardi, P.; Radó, J.; Straszner, A.; Ferencz, J.; Hajnal, Z.; Soleimani, S.; Schneider, M.; Schmid, U.; Révész, P.; Volk, J. Spiral-Shaped Piezoelectric MEMS Cantilever Array for Fully Implantable Hearing Systems. *Micromachines* **2017**, *8*, 311. [CrossRef]
195. Castagnetti, D.; Radi, E. A piezoelectric based energy harvester with dynamic magnification: Modelling, design and experimental assessment. *Meccanica* **2018**, *53*, 2725–2742. [CrossRef]
196. Aldraihem, O.; Baz, A. Energy Harvester with a Dynamic Magnifier. *J. Intell. Mater. Syst. Struct.* **2011**, *22*, 521–530. [CrossRef]
197. Ma, P.; Kim, J.E.; Kim, Y.Y. Power-amplifying strategy in vibration-powered energy harvesters. *Proc. SPIE Int. Soc. Opt. Eng.* **2010**, *76430O* . [CrossRef]
198. Aladwani, A.; Aldraihem, O.; Baz, A. A Distributed Parameter Cantilevered Piezoelectric Energy Harvester with a Dynamic Magnifier. *Mech. Adv. Mater. Struct.* **2014**, *21*, 566–578. [CrossRef]
199. Aladwani, A.; Arafa, M.; Aldraihem, O.; Baz, A. Cantilevered Piezoelectric Energy Harvester with a Dynamic Magnifier. *J. Vib. Acoust.* **2012**, *134*, 031004. [CrossRef]
200. Yang, Z.; Yang, J. Connected Vibrating Piezoelectric Bimorph Beams as a Wide-band Piezoelectric Power Harvester. *J. Intell. Mater. Syst. Struct.* **2009**, *20*, 569–574. [CrossRef]
201. Dong, L.; Closson, A.B.; Oglesby, M.; Escobedo, D.; Han, X.; Nie, Y.; Huang, S.; Feldman, M.D.; Chen, Z.; Zhang, J.X. In vivo cardiac power generation enabled by an integrated helical piezoelectric pacemaker lead. *Nano Energy* **2019**, *66*, 104085. [CrossRef]
202. Kim, M.; Yun, K.S. Helical Piezoelectric Energy Harvester and Its Application to Energy Harvesting Garments. *Micromachines* **2017**, *8*, 115. [CrossRef]
203. Arul, A.; Rajan, S. Efficiency Evaluation of a MOSFET bridge rectifier for Powering LEDs using Piezo-electric Energy Harvesting Systems. *Automatika* **2016**, *57*, 329–336. [CrossRef]
204. Le, T.; Han, J.; von Jouanne, A.; Mayaram, K.; Fiez, T. Piezoelectric micro-power generation interface circuits. *IEEE J. Solid-State Circuits* **2006**, *41*, 1411–1420. [CrossRef]
205. Erturk, A.; Inman, D.J. A Brief Review of the Literature of Piezoelectric Energy Harvesting Circuits. In *Piezoelectric Energy Harvesting*; John Wiley & Sons, Ltd.: Hoboken, NJ, USA, 2011; Chapter 11, pp. 325–342. [CrossRef]
206. Badel, A.; Guyomar, D.; Lefeuvre, E.; Richard, C. Efficiency Enhancement of a Piezoelectric Energy Harvesting Device in Pulsed Operation by Synchronous Charge Inversion. *J. Intell. Mater. Syst. Struct.* **2005**, *16*, 889–901. [CrossRef]
207. Richard, C.; Guyomar, D.; Audigier, D.; Ching, G.K. Semi-passive damping using continuous switching of a piezoelectric device. In Proceedings of the Smart Structures, Newport Beach, CA, USA, 1–3 March 1999.
208. Guyomar, D.; Badel, A.; Lefeuvre, E.; Richard, C. Toward energy harvesting using active materials and conversion improvement by nonlinear processing. *IEEE Trans. Ultrason. Ferroelectr. Freq. Control* **2005**, *52*, 584–595. [CrossRef]
209. Badel, A.; Benayad, A.; Lefeuvre, E.; Lebrun, L.; Richard, C.; Guyomar, D. Single crystals and nonlinear process for outstanding vibration-powered electrical generators. *IEEE Trans. Ultrason. Ferroelectr. Freq. Control* **2006**, *53*, 673–684. [CrossRef]
210. Liang, J.; Liao, W.H. Piezoelectric Energy Harvesting and Dissipation on Structural Damping. *J. Intell. Mater. Syst. Struct.* **2009**, *20*, 515–527. [CrossRef]
211. Wu, L.; Do, X.D.; Lee, S.G.; Ha, D.S. A Self-Powered and Optimal SSHI Circuit Integrated With an Active Rectifier for Piezoelectric Energy Harvesting. *IEEE Trans. Circuits Syst. I Regul. Pap.* **2017**, *64*, 537–549. [CrossRef]
212. Liu, H.; Hua, R.; Lu, Y.; Wang, Y.; Salman, E.; Liang, J. Boosting the efficiency of a footstep piezoelectric-stack energy harvester using the synchronized switch technology. *J. Intell. Mater. Syst. Struct.* **2019**, *30*, 1045389X1982851. [CrossRef]
213. Lallart, M.; Guyomar, D. An optimized self-powered switching circuit for non-linear energy harvesting with low voltage output. *Smart Mater. Struct.* **2008**, *17*, 035030. [CrossRef]
214. Du, S.; Jia, Y.; Do, C.D.; Seshia, A.A. An Efficient SSHI Interface With Increased Input Range for Piezoelectric Energy Harvesting Under Variable Conditions. *IEEE J. Solid-State Circuits* **2016**, *51*, 2729–2742. [CrossRef]
215. Lefeuvre, E.; Badel, A.; Richard, C.; Guyomar, D. Piezoelectric Energy Harvesting Device Optimization by Synchronous Electric Charge Extraction. *J. Intell. Mater. Syst. Struct.* **2005**, *16*, 865–876. [CrossRef]
216. Cai, Y.; Manoli, Y. A piezoelectric energy harvester interface circuit with adaptive conjugate impedance matching, self-startup and 71% broader bandwidth. In Proceedings of the ESSCIRC 2017—43rd IEEE European Solid State Circuits Conference, Leuven, Belgium, 11–14 September 2017; pp. 119–122. [CrossRef]

217. Lefeuvre, E.; Badel, A.; Brenes, A.; Seok, S.; Yoo, C.S. Power and frequency bandwidth improvement of piezoelectric energy harvesting devices using phase-shifted synchronous electric charge extraction interface circuit. *J. Intell. Mater. Syst. Struct.* **2017**, *28*, 1045389X1770491. [CrossRef]
218. Shareef, A.; Goh, W.L.; Narasimalu, S.; Gao, Y. A Rectifier-Less AC–DC Interface Circuit for Ambient Energy Harvesting From Low-Voltage Piezoelectric Transducer Array. *IEEE Trans. Power Electron.* **2019**, *34*, 1446–1457. [CrossRef]
219. Wang, X.; Zha, X.; Tu, Y.; Shi, G.; Ye, Y.; Xia, Y. A synchronous charge extraction piezoelectric energy harvesting circuit based on precision active control peak detection with supplement energy. In Proceedings of the 2017 IEEE 12th International Conference on ASIC (ASICON), Guiyang, China, 25–28 October 2017; pp. 275–278. [CrossRef]
220. Hehn, T.; Hagedorn, F.; Maurath, D.; Marinkovic, D.; Kuehne, I.; Frey, A.; Manoli, Y. A Fully Autonomous Integrated Interface Circuit for Piezoelectric Harvesters. *IEEE J. Solid-State Circuits* **2012**, *47*, 2185–2198. [CrossRef]
221. Xu, S.; Ngo, K.D.T.; Nishida, T.; Chung, G.B.; Sharma, A. Low Frequency Pulsed Resonant Converter for Energy Harvesting. *IEEE Trans. Power Electron.* **2007**, *22*, 63–68. [CrossRef]
222. Kwon, D.; Rincon-Mora, G. A single-inductor AC-DC piezoelectric energy-harvester/battery-charger IC converting ±(0.35 to 1.2 V) to (2.7 to 4.5 V). In Proceedings of the 2010 IEEE International Solid-State Circuits Conference—(ISSCC), San Francisco, CA, USA, 7–11 February 2010; Volume 53, pp. 494–495. [CrossRef]
223. Hehn, T.; Hagedorn, F.; Manoli, Y. Highly Efficient Energy Extraction from Piezoelectric Generators. *Procedia Chem.* **2009**, *1*, 1451–1454. [CrossRef]
224. Hehn, T.; Manoli, Y. *CMOS Circuits for Piezoelectric Energy Harvesters*; SpringerLink: Berlin/Heidelberg, Germany, 2014.
225. Xu, Q.; Gao, A.; Li, Y.; Jin, Y. Design and Optimization of Piezoelectric Cantilever Beam Vibration Energy Harvester. *Micromachines* **2022**, *13*, 675. [CrossRef] [PubMed]
226. Park, J.; Lee, D.H.; Park, J.Y.; Chang, Y.S.; Lee, Y.P. High performance piezoelectric MEMS energy harvester based on D33 mode of PZT thin film on buffer-layer with PBTIO3 inter-layer. In Proceedings of the TRANSDUCERS 2009—2009 International Solid-State Sensors, Actuators and Microsystems Conference, Denver, CO, USA, 21–25 June 2009; pp. 517–520. [CrossRef]
227. Kim, H.; Kim, S.M.; Son, H.; Kim, H.; Park, B.; Ku, J.; Sohn, J.I.; Im, K.; Jang, J.E.; Park, J.J.; et al. Enhancement of piezoelectricity via electrostatic effects on a textile platform. *Energy Environ. Sci.* **2012**, *5*, 8932–8936. [CrossRef]
228. Elfrink, R.; Kamel, T.M.; Goedbloed, M.; Matova, S.; Hohlfeld, D.; van Andel, Y.; van Schaijk, R. Vibration energy harvesting with aluminum nitride-based piezoelectric devices. *J. Micromech. Microeng.* **2009**, *19*, 094005. [CrossRef]
229. Pi, Z.; Zhang, J.; Wen, C.; bin Zhang, Z.; Wu, D. Flexible piezoelectric nanogenerator made of poly(vinylidenefluoride-co-trifluoroethylene) (PVDF-TrFE) thin film. *Nano Energy* **2014**, *7*, 33–41. [CrossRef]
230. Güçlü, H.; Kasım, H.; Yazici, M. Investigation of the optimum vibration energy harvesting performance of electrospun PVDF/$BaTiO_3$ nanogenerator. *J. Compos. Mater.* **2023**, *57*, 409–424. [CrossRef]
231. Zhang, Y.; Jeong, C.K.; Yang, T.; Sun, H.; Chen, L.Q.; Zhang, S.; Chen, W.; Wang, Q. Bioinspired elastic piezoelectric composites for high-performance mechanical energy harvesting. *J. Mater. Chem. A* **2018**, *6*, 14546–14552. [CrossRef]
232. Zhu, J.; Jia, L.; Huang, R. Electrospinning poly(l-lactic acid) piezoelectric ordered porous nanofibers for strain sensing and energy harvesting. *J. Mater. Sci. Mater. Electron.* **2017**, *28*, 12080–12085. [CrossRef]
233. Zheng, Q.; Zhang, H.; Mi, H.; Cai, Z.; Ma, Z.; Gong, S. High-performance flexible piezoelectric nanogenerators consisting of porous cellulose nanofibril (CNF)/poly(dimethylsiloxane) (PDMS) aerogel films. *Nano Energy* **2016**, *26*, 504–512. [CrossRef]